SEMIANNUAL REPORT

FOR

SOLAR CELL RESEARCH

(PHASE II)

Prepared Under:

WORK ORDER 8056

NAS 7-100

Prepared By:

R. L. Statler
N. D. Wilsey
J. E. Stannard
R. J. Lambert

Naval Research Laboratory
Solid State Applications Branch
Washington, D. C. 20390

15 April 1970

SEMIANNUAL REPORT

FOR

SOLAR CELL RESEARCH (PHASE II)

Work Done By:

R. L. Statler
J. E. Stannard
N. D. Wilsey
R. J. Lambert
J. A. Pfaff

Report Written By:

R. L. Statler
J. E. Stannard
N. D. Wilsey
R. J. Lambert

Prepared by

Naval Research Laboratory
Solid State Applications Branch
Washington, D. C. 20390

Under Work Order 8056

This work was performed for the Jet Propulsion Laboratory, California Institute of Technology, as sponsored by the National Aeronautics and Space Administration under Contract NAS 7-100.

This report contains information prepared by the Naval Research Laboratory under JPL sub-contract. Its content is not necessarily endorsed by the Jet Propulsion Laboratory, California Institute of Technology, or by the National Aeronautics and Space Administration.

R. L. Statler
Program Manager

E. L. Brancato
Project Supervisor

ABSTRACT

This report covers six months of progress which delineates the radiation behavior of silicon silar cells and lithium-doped silicon. Two major topics are investigated: (1) the effectiveness of lithium dopant in diminishing permanent radiation damage in silicon solar cells, and (2) the influence of cryogenic temperature environment on electron radiation damage in silicon solar cells.

In an effort to improve the quality of Si(Li) Hall samples, an extra etching process introduced in the diffusion schedule results in lithium concentrations which are well-controlled and specified to within 40%. By other techniques, the homogeneity of the lithium profile in the wafer is improved 4-fold to within a 50% variation.

The carrier removal rates of various distinguishable radiation-formed acceptor levels was measured in 6 Ω- cm lithium-doped and 14 Ω- cm phosphorus-doped float-zone silicon. It was found that 1 MeV electron irradiation at 240°K in both types of crystals results in nearly the same carrier removal rates both for E centers (impurity-vacancy) and a center at E_c-0.12 eV. However, the lithium-doped material has a total carrier removal rate three times greater than that in phosphorus-doped silicon. Hall measurements suggested that this is caused by a deep acceptor center related to the presence of a neutral phase of lithium in the crystal.

A Cobalt-60 gamma irradiation of lithium-doped and n/p solar cells was carried out to an equivalent fluence of 0.93×10^{14} 1 MeV e/cm^2. The equivalent flux rate is $\sim 5 \times 10^6$ e/cm^2-sec. Although the degradation rate of the relative maximum power is markedly less for one group (H9) of float-zone lithium cells, than any other, the absolute power output of all lithium cells is less than the n/p cells, because of their lesser initial efficiencies. All cells irradiated at 60°C show greater damage than the ones irradiated at 30°C.

Some of the unirradiated control cells, notably the n/p and float-zone lithium, which were illuminated and stored at 60°C, degraded slightly in power output, indicating the action of a damage mechanism other than radiation.

The temperature-dependence of 1 MeV electron damage in n/p solar cells was studied for a set of 10 Ω- cm cells, all fabricated from the same boule of quartz-crucible silicon. The damage rate (as indicated by the loss of short-circuit current with fluence) is much more dependent on the measurement temperature than on the temperature of irradiation.

Cells irradiated to a fluence of 5×10^{15} e/cm^2 at 300°K show a degradati of 39 percent when measured at 90°K but only lose 27 percent of their pre-irr short-circuit current when measured at 300°K. Cells irradiated at 125 °K and sured at 90°K have a decrease of 35 percent. This indicates that during irra stable defects are formed which have a temperature-dependent charge state.

CONTENTS

ILLUSTRATIONS

TABLES

1.0 INTRODUCTION

This report describes the progress during the six month period from 7 October 1969 to 7 April 1970. The work performed under this contract is a continuation of that which was begun in October 1968 under Work Order 8056 from the Jet Propulsion Laboratory.

The program is directed toward improving the radiation resistance of silicon solar cells. In order to progress to this objective most efficiently, we are increasing our understanding in specific areas of how radiation interacts with the solar cell. Based on this new body of knowledge, suggestions and predictions can be made for improved solar cell structures. The particular areas of study include investigating radiation effects in lithium-diffused silicon crystals, the measurement and evaluation of the properties of manufactured lithium solar cells, and the radiation effects on solar cells as a function of temperature and illumination.

The objective of the silicon crystal study is to understand the radiation-damage effects in lithium-diffused solar cells. This can only be accomplished when the multiple interactions of lithium in silicon are defined. The approach to this task is to utilize the measurement of Hall coefficient in irradiated lithium-diffused silicon as a function of temperature, fluence, and post-irradiation thermal annealing time. The unique feature of the Hall measurement as a function of temperature between $4^{\circ}K$ and $300^{\circ}K$ is that a separate determination of acceptor and donor concentrations can be made in materials where one type of each is present.

Another aspect of the effect of lithium in silicon is being investigated. This is a unique experiment which evaluates the photovoltaic properties of manufactured lithium-doped solar cells functioning under illumination and subjected to irradiation at a level comparable to space flux. Sixty-five cells are irradiated by Cobalt-60 gamma rays at two temperatures in a statistically-designed experiment. Data has been obtained over a seven month period to a dose approximately equivalent to 1×10^{14} 1 MeV e/cm^2.

The last section of the program is concerned with measuring the effect of radiation on silicon solar cells at low temperatures. In conjunction with low-temperature irradiations, the photovoltaic properties are also measured at low temperatures as a function of intensity of illumination. This information is urgently required as a basis for designing solar arrays for outer planetary missions. Cell temperatures at least as low as $125^{\circ}K$ and illumination intensities as small as $5\,mW/cm^2$ are achieved.

2.0 DISCUSSION

2.1 Hall Effect Studies in Lithium-Diffused Silicon

2.1.1 Introduction. The purpose of this work is to follow the events that occur during electron damage and room-temperature recovery in float-zone silicon doped with lithium. Cryogenic Hall measurements to 10°K enable the overall concentration of radiation-induced deep acceptors to be monitored independently, along with the overall concentration of shallow donors. In addition, the activation energy and concentration of levels lying between E_c-0.06 and E_c-0.20 eV may be separately measured, provided the spectrum is not too complex. A valid interpretation of the Hall data strongly depends on using Hall samples which are lithium-diffused homogenously and have the correct activation energy for the lithium donor level.

2.1.2 Sample Preparation. During the past 6 months, the preparation and characterization of lithium-doped silicon have been greatly improved. In particular, three problems associated with preparation of lithium doped material were attacked and essentially solved. These were: (1) the effect of inhomogeneity on Hall measurements, (2) methods of obtaining material displaying the proper activation energy for lithium, and (3) a good method of controlling lithium concentration.

In this study, lithium has been introduced by diffusion from a suspension of lithium in oil. A "tack-on" treatment of 5 minutes at 425°C followed by a 60 minute redistribution at the same temperature has been employed. Control of the final lithium concentration can be effected by controlling the number of lithium atoms present in the surface layers of the sample at the start of redistribution. Etching in CP-4 allows a thickness controllable to within $\pm 10^{-4}$ inches to be removed, thereby reducing the overall lithium content. Figure 1 shows the results of a four-point probe study of samples prepared using these techniques. The lithium concentration measured after redistribution is shown to decrease uniformly as the thickness etched away before redistribution is made larger. The use of starting material with a resistivity greater than 100 Ω - cm would allow this number to be reduced to even lower values. A set of six samples was made to indicate the batch reproducibility of this method. Most of the spread in data is due to variations in the amount of lithium applied to each slice before the "tack-on" treatment. It is of interest to note that the final lithium concentration was not dependent upon the initial thickness of the silicon wafer.

Another difficulty arising from lithium diffusion from an oil suspension is the resultant inhomogenous lithium concentration having a minimum value at the surface. Figure 2 shows the degree of this inhomogeneity and its effect on Hall measurements, as well as the improvement in concentration homogeneity which this controlled etch process affords. Curve I exhibits four-point probe data

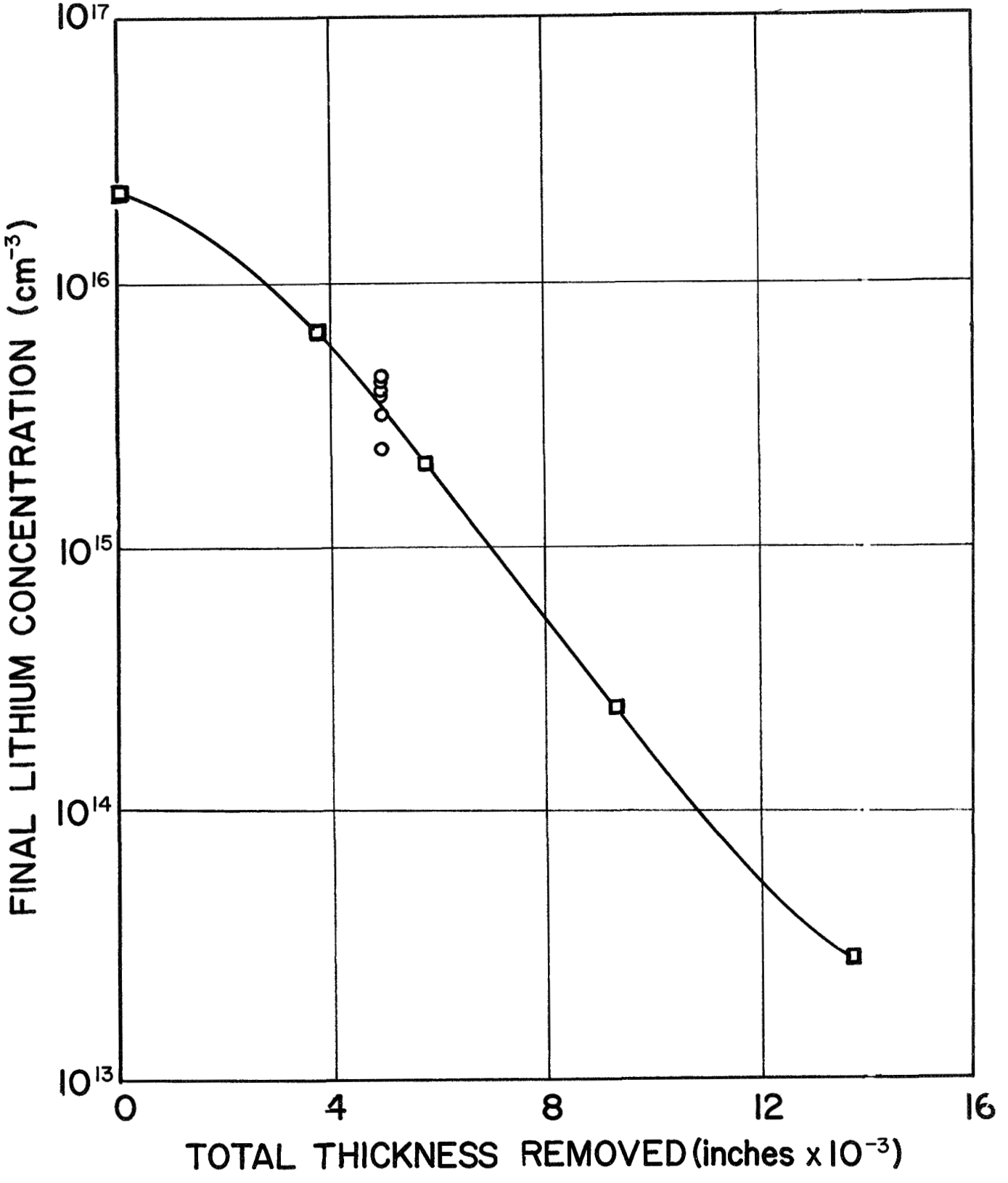

Fig. 1 - Reproducible control of lithium concentrations by means of etching prior to redistribution.

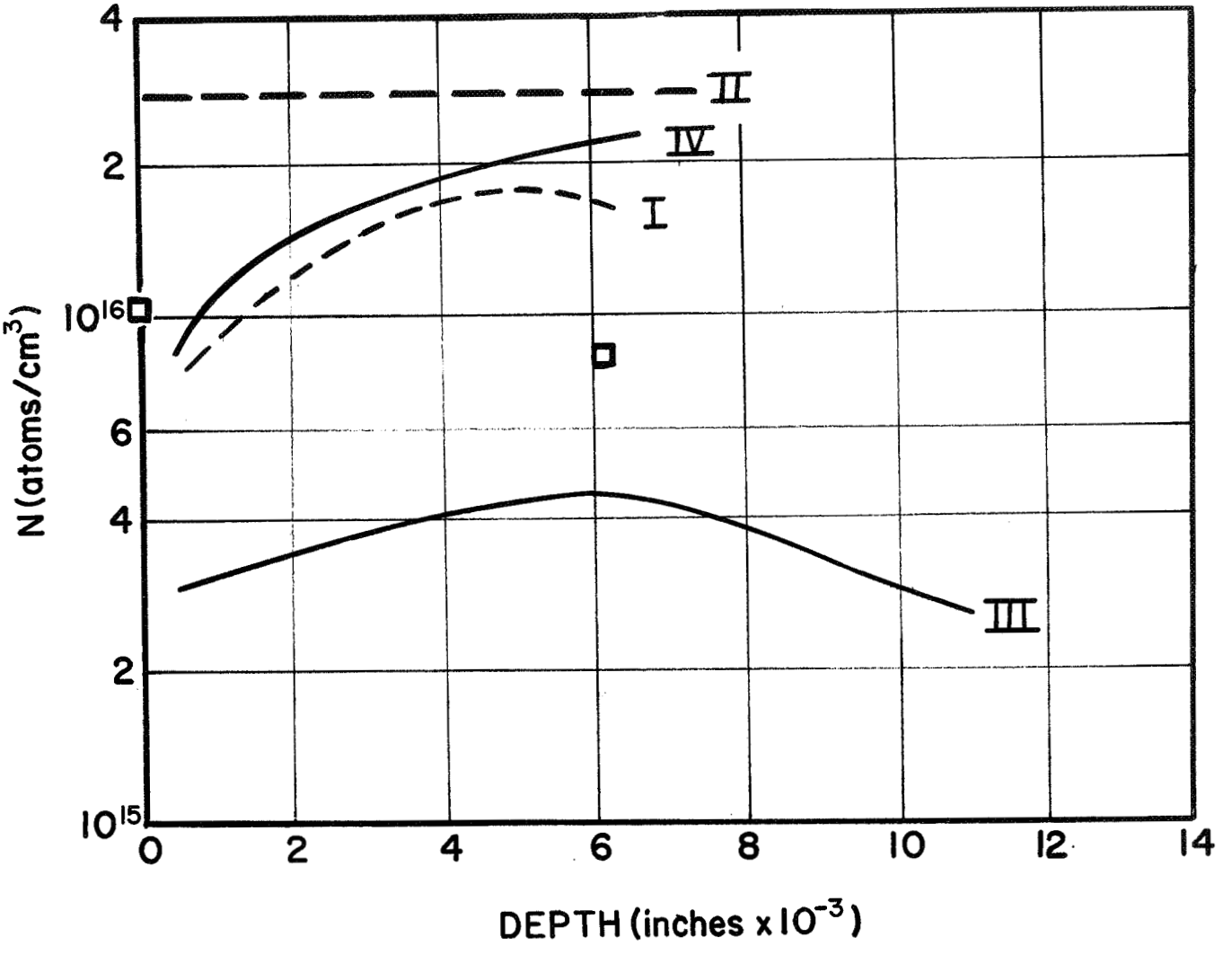

Fig. 2 - Inhomogeneity of lithium concentration -

I. Heliotek data by 4 point probe; (5/425 - 60/425) treatment

II. The uniform lithium concentration expected in the Heliotek sample had there been no lithium lost during redistribution

III. Four point probe measurements on a sample etched prior to redistribution (5/425 - etch - 60/425)

IV. Hall bridge resistivity measurements on a sample redistributed with lapped surfaces. (6/425 - Lap - 60/425)

□ Hall measurements on the sample of curve IV.

taken by Heliotek.[1] Graphical integration of this and other Heliotek data indicates that a one hour redistribution at 425°C causes the total amount of active lithium contained in a sample to decrease to 30% of its initial value. The magnitude of this decrease is independent of the amount of lithium introduced by the particular "tack-on" treatment used. Curve II indicates the lithium concentration expected for the sample of Curve I had there been no redistribution loss. Outgassing, surface precipitation, and distributed precipitation can all contribute to this loss. Curve III is a four-point probe profile of a sample prepared in such a way as to minimize inhomogeneity. Lithium was applied to both surfaces of the wafer and followed by a "tack-on" of five minutes at 425°C. After etching to reduce the lithium content, it was redistributed for one hour at 425°C. This profile shows the sample was homogenous to within about 50%. The irradiation study to be described was performed on material prepared in this way, except for an additional 0.002 inch etch after redistribution in order to remove possible surface precipitates.

The effect of inhomogeneity on Hall measurements is indicated by results obtained from the sample of Curve IV. Curve IV shows the carrier concentration as determined by resistivity measurements on a Hall bridge, while the square data-points indicate carrier concentration as obtained from the Hall effect. It is apparent that the Hall effect is strongly influenced by the high resistivity portion of the sample near the surface, due to the larger Hall voltage generated there. The second point is at a lower value than the first, in anticipation of a decrease in lithium concentration which occurs with increasing depth.

Such inhomogeneity can affect more than the apparent lithium concentration. It can lead to erroneous values for the activation energy at the lithium donor level. The sample of Curve IV had been redistributed with a lapped surface and showed a low temperature activation energy of 0.0374 eV, which is the energy of the LiO complex. Surface damage apparently caused complete precipitation of free lithium in the region near the surface, thereby leaving the LiO complex as the shallowest active donor present. This would cause the low-temperature resistivity in this region to exceed that of the lithium-doped bulk by orders of magnitude. As a result, the electrical properties of the sample were dominated by the high resistivity surface region. Redistribution after etching the surfaces in CP-4 avoids this condition. In the past, some samples have shown activation energies as low as 0.026 eV. This was apparently due to contamination of the lithium-oil suspension. Two samples produced and measured after changing to a new suspension have shown energies of 0.0331 eV and 0.0332 eV. Thermal and optical values of 0.033[2] and 0.03281[3] eV respectively are reported for more heavily doped material, and would be expected to be smaller than our value due to impurity overlap effects.

2.1.3 Analysis of Hall Data by Computer. Before considering irradiation experiments, it is appropriate to discuss data analysis and what kind of information is obtained. Both Hall constant and resistivity have been measured as a function of temperature, thereby giving the temperature dependence of the carrier concentration and mobility. A program for the calculation of Hall mobility in silicon from first principles has not been written as yet, so carrier mobility will not be treated here. Figure 3 is a picture of the carrier concentration as a function of temperature, along with a diagram of the forbidden gap of silicon. The states shown in the diagram would give rise to this general form of the carrier concentration. From the location of the plateau at 100°K and the location of the linear "freeze out" region, we can calculate the overall donor concentration along with the number of deep acceptors. The slope of the linear region gives directly the energy separation between the lithium donor and the bottom of the conduction band. Analysis of the high temperature structure (near 300°K) can give the concentration and energy of a level lying more than 0.06 eV and less than 0.2 eV below the conduction band edge. The difference between the plateaus at 300°K and at 100°K gives the concentration of such a level. The position of the transition between the two plateaus gives the activation energy. In the case of unirradiated lithium-doped silicon, the data between 50°K and 100°K allows the lithium and phosphorus concentrations to be determined separately with moderate success even though their energy separation is only 0.011 eV. Models including excited states, however, gave poorer fits to the data for both phosphorus and lithium-doped materials.

For each sample, a least-squares fit to the data was obtained for temperatures below 100°K. If a level of intermediate depth was present, these results were then used to aid in obtaining a separate fit to data above 100°K. Figure 4 shows the results of this fitting process for an unirradiated phosphorus-doped sample and an unirradiated sample containing both phosphorus and lithium. The first two columns show the results obtained using four adjustable parameters. The last column used a five-parameter model in order to allow separate determination of the lithium and phosphorus concentrations. The indicated errors are 95% confidence limits, and the bottom row shows the mean error between calculated and measured values of the carrier concentration. In the first column, the measured value of the phosphorus ground-state degeneracy is quite close to the theoretical value of 0.50. The measured value of the activation energy agrees closely with the reported optical ionization energy of 0.0453 eV[3,4]. Equally reliable values of the parameters are obtained for the lithium doped sample in the second column. The measured activation energy of 0.0332 eV is slightly larger than the reported optical value 0.03281 eV, as expected. The five-parameter model which most accurately represents this sample gives a degeneracy factor close to the expected value of 0.1. The close correspondence between calculated and theoretical values of the degeneracy factor for both lithium and phosphorus lends considerable support to the confidence one has that the values of the other parameters truly reflect the properties of the sample. Large errors shown for the donor concentrations would have been much less had more data been taken between 50°K and

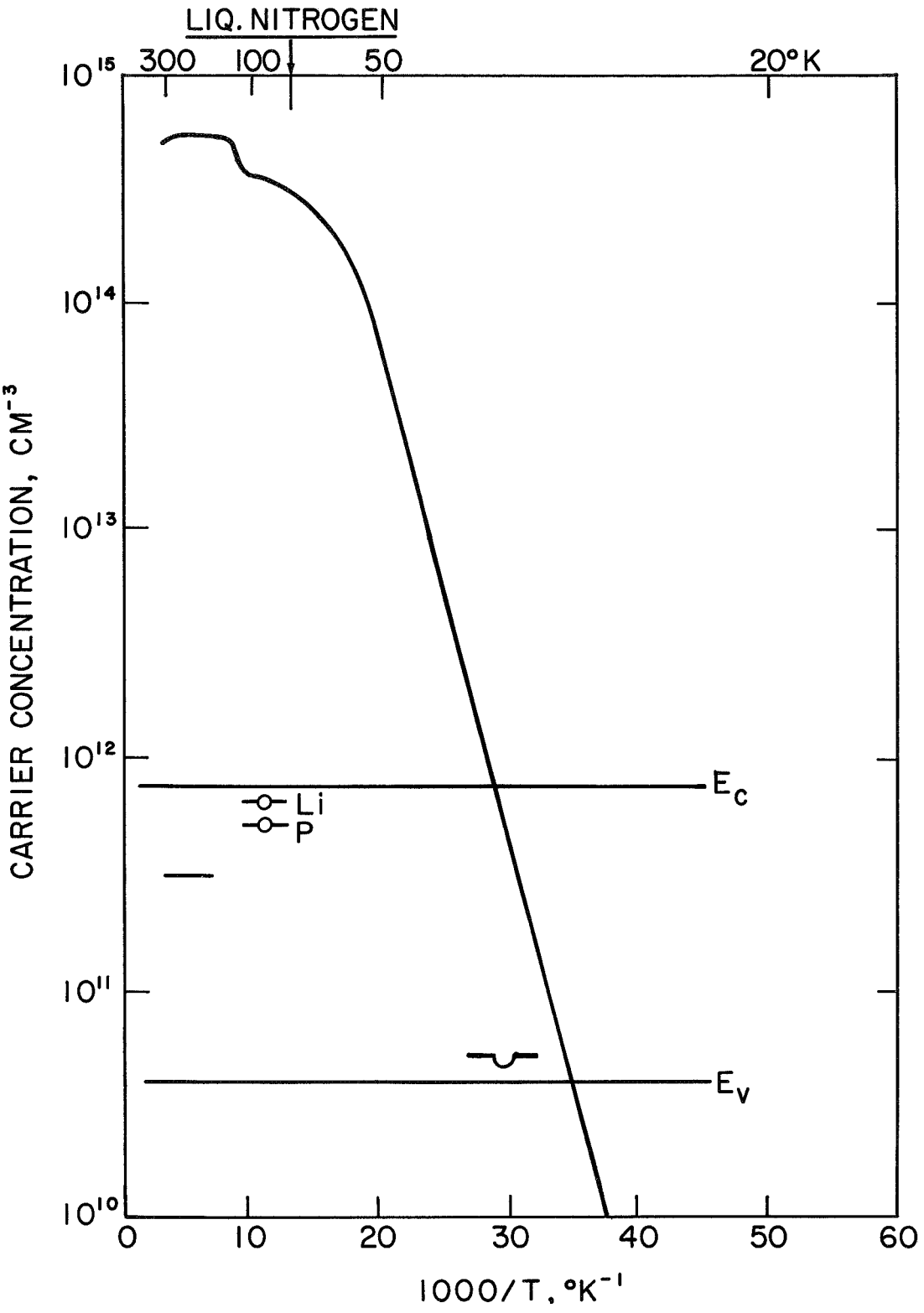

Fig. 3 - Information obtainable from Hall measurements as a function of temperature. The densities and ionization energies of the states shown in the forbidden gap can be determined with the restrictions explained in the text.

PARAMETER	Si (P) 4 PARAMETERS	Si (Li) 4 PARAMETERS	Si (Li, P) 5 PARAMETERS
PHOSPHORUS CONCENTRATION	$3.26 \pm 0.07 \times 10^{14}$ CM^{-3}	$6.8 \pm 0.2 \times 10^{14}$ CM^{-3}	$2.2 \pm 2.0 \times 10^{14}$ CM^{-3}
LITHIUM CONCENTRATION			$5.0 \pm 2.0 \times 10^{14}$ CM^{-3}
DONOR GROUND STATE DEG. FACTOR	0.55 ± 0.04	0.063 ± 0.005	0.10 ± 0.04
ACCEPTOR CONCENTRATION	$7.9 \pm 0.8 \times 10^{12}$ CM^{-3}	$5.4 \pm 0.6 \times 10^{12}$ CM^{-3}	$5.5 \pm 0.6 \times 10^{12}$ CM^{-3}
DONOR ACTIVATION ENERGY	0.0452 ± 0.0002 eV	0.0332 ± 0.0002	0.0332 ± 0.0002
STANDARD DEVIATION	1.3 %	1.4 %	1.3 %

Fig. 4 - Parameters obtained by fitting various models to data taken from unirradiated Si(P) and Si(Li,P).

100 °K. Since irradiation causes a noticeable worsening of the fits obtainable, only the four parameter model was used in irradiation studies. The measured donor concentration is then taken as equal to the sum of the concentrations of the individual donors. A similar interpretation is given the measured acceptor concentration.

2.1.4 Electron Radiation Experiments. In order to separate in time the events associated with damage, from those associated with annealing, irradiations were performed at a low enough temperature where lithium is immobile in silicon. Two experiments were planned and carried out. The first experiment was designed to discover whether lithium was associated with the level of intermediate depth (E_c -0.12) reported last year, using an 80°K irradiation. The second experiment involves irradiation at 240°K and subsequent room-temperature annealing of silicon doped with 5×10^{14} lithium/cm^3.

(A) Radiation at 80°K.

An earlier experiment showed that a level of intermediate depth was present following 80°K bombardment and extensive room temperature annealing of silicon lightly doped with lithium.* In the present experiment, a sample from the same phosphorus-doped starting material was measured before and after an 80°K irradiation by 5×10^{13} 1 MeV electrons/cm^2. The samples were annealed isochronally to a temperature of 200°K, and the temperature dependence of the carrier concentration was measured above 80°K. Figure 5 shows an intermediate level which was observed in irradiated and annealed phosphorus-doped material as well as irradiated and annealed lithium-doped material. The curves shown are data-fitted by computer using a model with three adjustable parameters. While a level is observed in the sample containing no lithium, its energy is definitely less than that measured in the lithium-doped sample. Very similar but more complete evidence obtained from the next experiment indicates that the association of mobile lithium with the 0.12 eV level causes a shift in its activation energy.

The identity of this 0.12 eV level in silicon is not known. Its energy lies close to the 0.13 eV value reported by H. Stein for a level formed following 80°K irradiation and 250°K annealing of pulled 10 Ω-cm silicon [5]. However, that experiment indicated the 0.13 eV level was not formed in float-zone silicon. This situation is further confounded by the fact that the present experiment indicates a removal rate in float-zone silicon roughly equal to the removal rate reported by Stein for pulled silicon.

(B) Radiation at 240°K

In the second experiment, two wafers were cut from a boule of 14 Ω-cm float-zone silicon. Lithium was diffused into one wafer to a resistivity of 6 Ω-cm using the techniques described in the first section. A full set of Hall measurements was made and each sample was irradiated at 240°K to a fluence of 1.7×10^{14} 1 MeV electrons/cm^2. The samples were remeasured without warming above 240°K.

*As reported by J. E. Stannard in the Annual Report for Solar Cell Research, W.O. 8056, NAS-7-100, NRL, 15 October 1969.

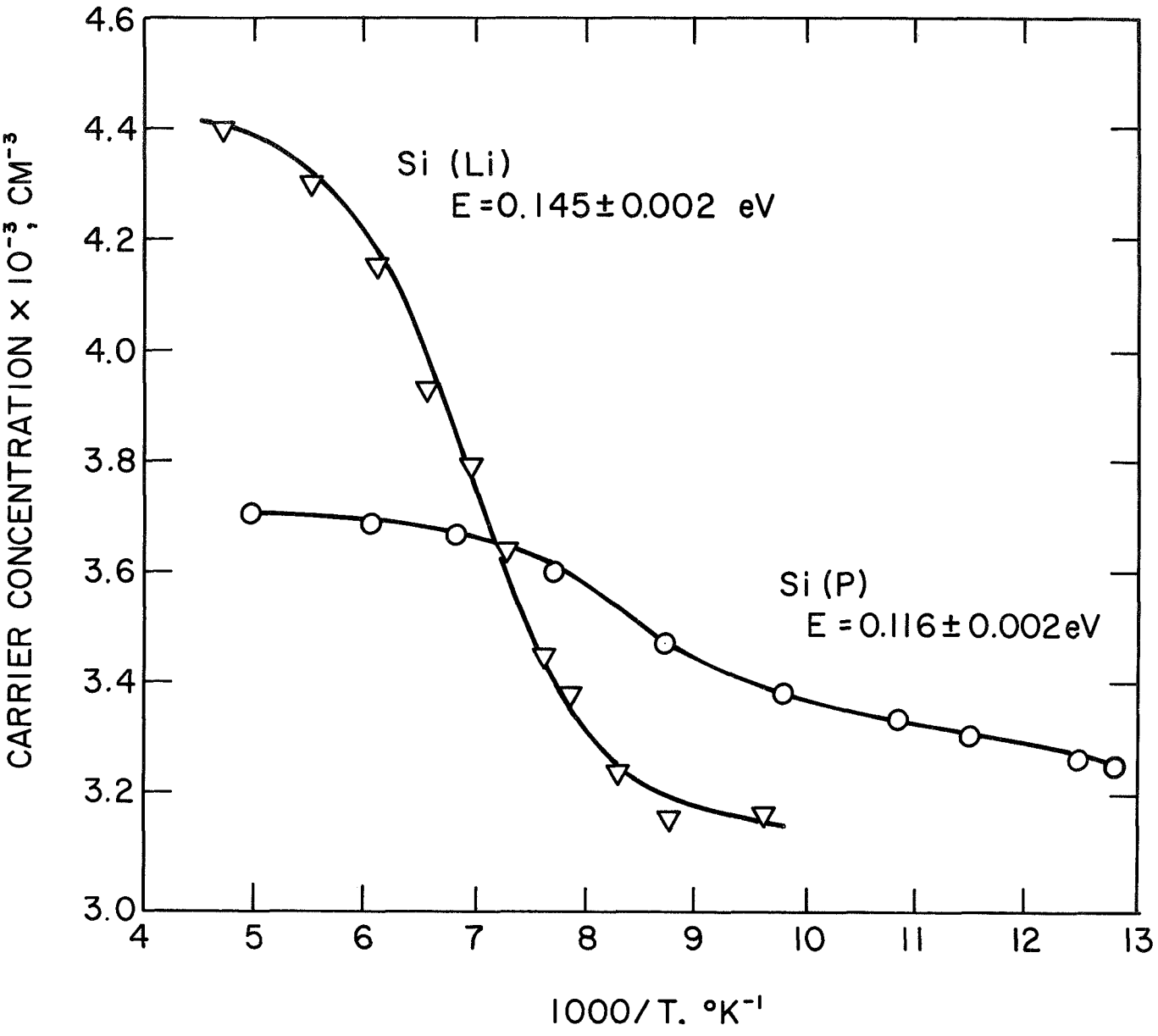

Fig. 5 - Radiation-induced intermediate level structure and least squares best fits for lithium and phosphorus-doped silicon

▽ 30 Ω cm-FZ Si(Li)

$\phi = 4 \times 10^{14}$ 1 MeV e/cm^2

$T_b = 80^{\circ}K$

$T_a = 300^{\circ}K$ for 1500 h.

0 100 Ω cm-FZ Si(P)

$\phi = 5 \times 10^{13}$ 1 MeV e/cm^2

$T_b = 80^{\circ}K$

$T_a = 200^{\circ}K$

Subsequent measurements were made after 2 hours and after 17 hours of annealing at room temperature. Irradiation was performed at 240°K where it was hoped that the 0.12 eV level might not form and yet the lithium ion would still be immobile. The results show that the 0.12 eV level was still formed, even at this temperature. Figure 6 shows the room-temperature annealing of carrier concentration frequently observed in irradiated lithium-doped silicon. The control sample as expected, shows no measurable annealing of the carrier concentration. Indexes on the horizontal axis refer to the annealing times at which full measurements were made.

Before considering results obtained after room-temperature annealing, we will consider the measurements made before and immediately after irradiation. E centers are formed when an electrically active donor interacts with a vacancy and that complex becomes a deep acceptor. In this experiment, such an event will cause the measured donor concentration to decrease by one and the acceptor concentration to increase by one. As a result, changes in electrically active donor concentration indicate directly the formation of E centers. Another point to be emphasized is that the measured value of overall acceptor concentration includes the E center concentration. Also, the 0.12 eV level is included because other experimental evidence indicates that it too is an acceptor. Figure 7 shows the carrier removal rates associated with E centers, overall acceptors, and the 0.12 eV level resulting from the irradiation of these samples. (At the time of this measurement no thermal annealing has occurred.) Carrier removal rate, shown on the vertical axis, equals the acceptor formation rate times the number of electronic charges a defect assumes in the material being considered. For example, the carrier removal rate and formation rate of the E center are equal since the E center is a singly ionized acceptor. The left side of Figure 7 is in agreement with present concepts of damage in float-zone phosphorus-doped silicon. Room-temperature irradiation of phosphorus-doped silicon produces nearly equal numbers of E centers, divacancies, and A centers as the primary damage centers [5]. It is somewhat surprising that no A centers were observed in these samples; however, no high-temperature structure with an activation energy near 0.17 eV was observed. This indicated that the A center concentration was considerably less than $5 \times 10^{12}/cm^3$. If the removal rate of the 0.12 eV center, which presumably would be replaced by a deeper level in a 300°K irradiation, is added to the rates shown for the two other defects, an overall carrier removal rate of 0.6 cm^{-1} is obtained. This compares well with a reported value of approximately 0.8 cm^{-1}.

The details of the electron damage are quite different in the case of the slice of silicon which was doped with 4×10^{14} lithium/cm^3. While the removal rates for the 0.12 eV level are comparable in the two samples, the lithium sample shows very little E center formation and a very large acceptor formation rate. There are two possible explanations for the fact that the concentration of electrically active lithium and phosphorus does not decrease as a result of the irradiation. One could presume that while vacancies still interact with and remove donors, there is another center introduced by the lithium diffusion which interacts with vacancies to

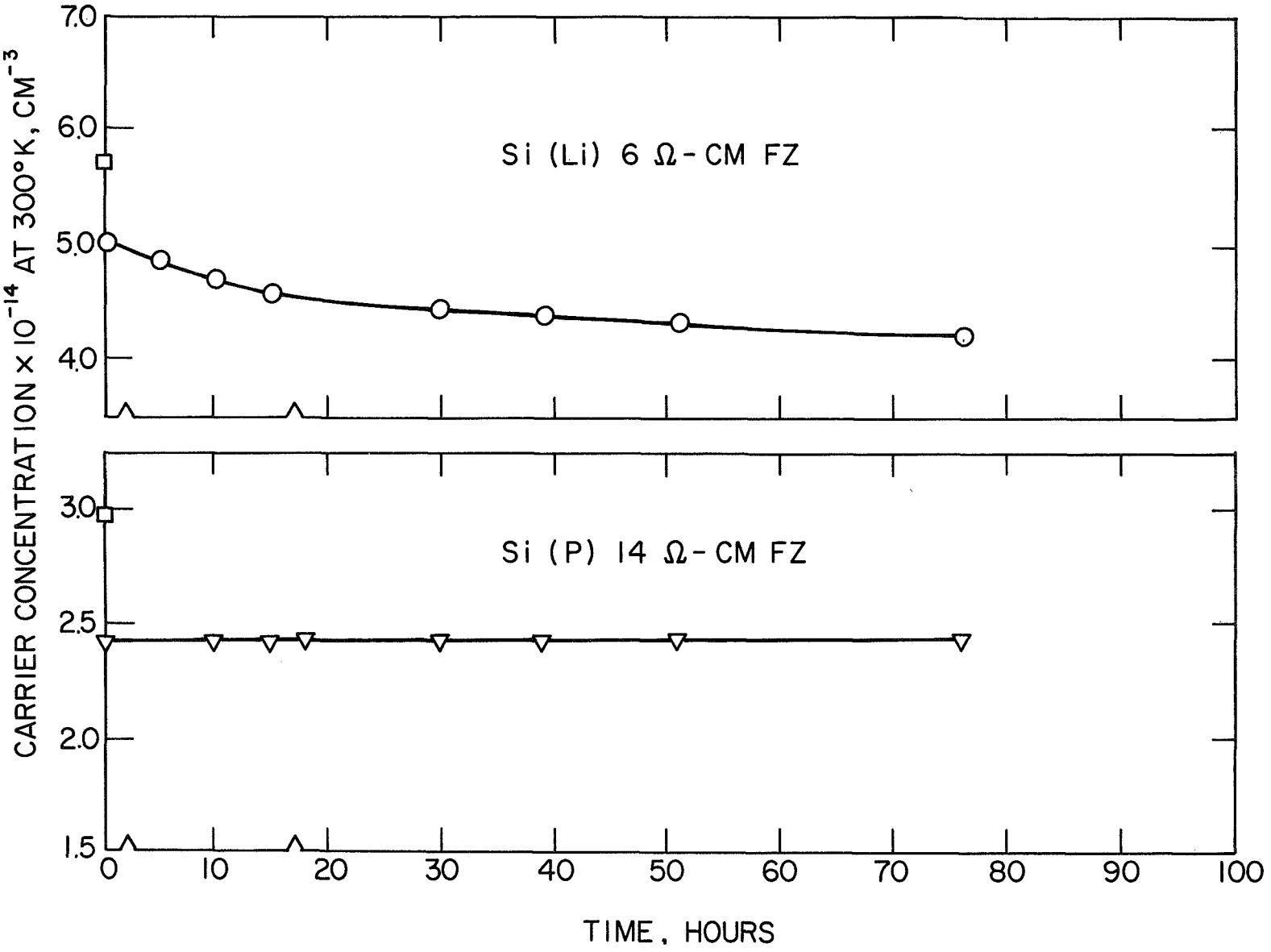

Fig. 6 - Annealing of room-temperature carrier concentration. Both the lithium-doped sample and its control was irradiated at 240°K by 1.7×10^{14} 1 MeV e/cm^2 and then allowed to anneal at room temperature

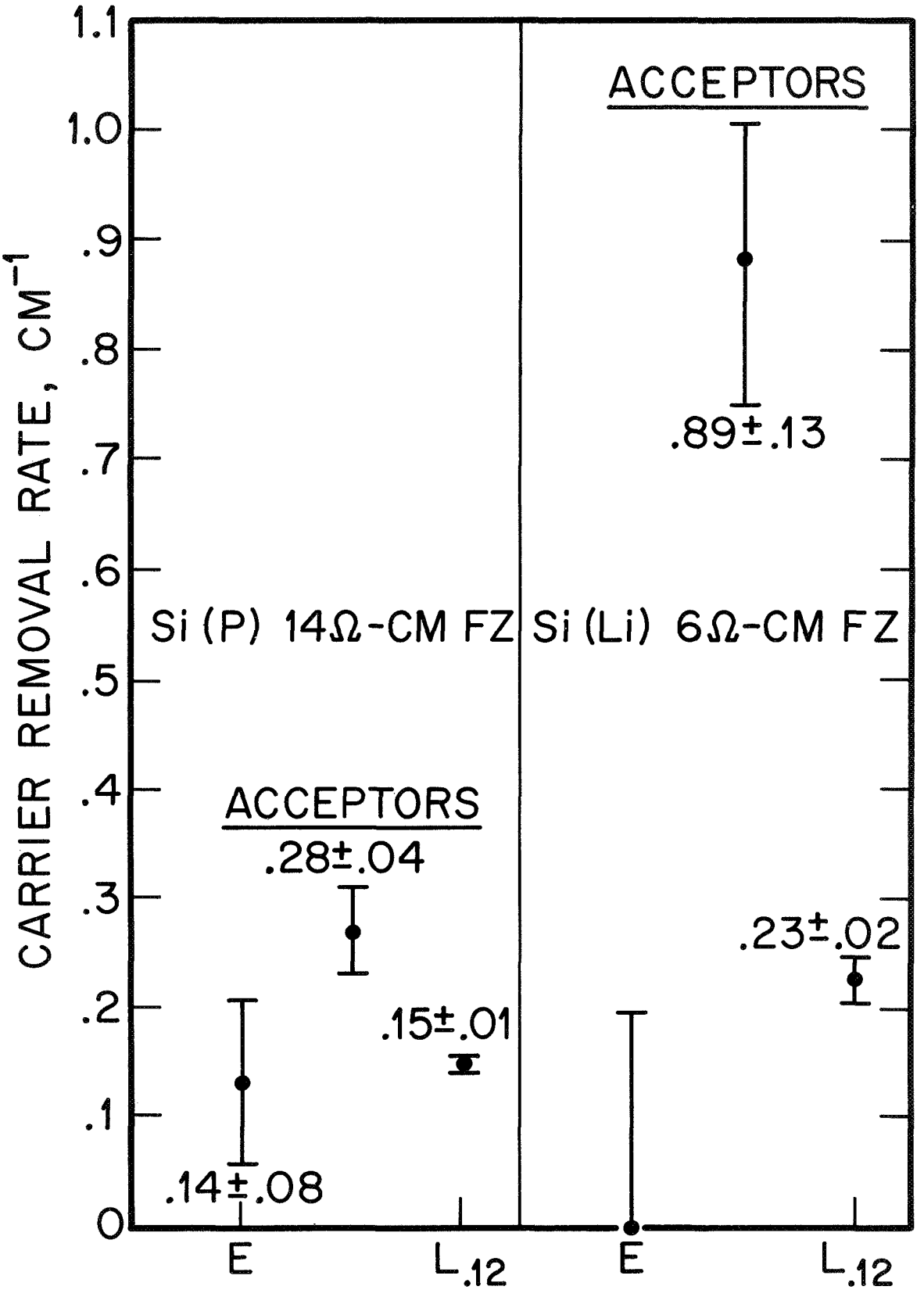

Fig. 7 - Radiation-induced changes in donor and acceptor concentration on lithium- and phosphorus-doped silicon. The samples of Fig. 4 were irradiated at 240°K and remeasured without allowing the lithium to become mobile.

form an equal number of new donors. The requirement of approximate equality between these two rates weakens the plausibility of this argument.

A more credible explanation is the following: diffusion of lithium into the sample introduces some initially undetectable center, that is, a neutral one, which acts as a very efficient "sink" for vacancies, removing them from the crystal before they have a chance to encounter a donor. The large magnitude of the acceptor generation would then seem to support this explanation.

Let us assume that there is a competition for vacancies between donors and, say, dislocations in the phosphorus-doped sample. Let us also assume that a vacancy is destroyed when it interacts with a dislocation. In the lithium-doped sample, the very efficient sink for vacancies that we have assumed would not only prevent vacancies from interacting with E centers, it would also trap vacancies normally destroyed at a dislocation. If it is presumed that these neutral centers form an acceptor upon trapping a vacancy, we see that an abnormally large formation rate for acceptors would be expected.

While the details of this explanation are speculative, it does seem that some neutral center involving lithium is present and affects the way damage is occuring in this sample. Such neutral centers might form during the redistribution phase, and could account for a part of the lithium lost during redistribution. No evidence of an energy level due to the acceptors was found from the Hall measurements. Thus the level must lie more than 0.2 eV below the conduction band.

Photoconductivity at 6.5^{o}K was measured out to 14 microns in these samples before and after irradiation. The photoconductive response was characteristic of that expected for a shallow impurity in silicon. Structure superimposed upon the impurity response did not correlate well with lattice absorption bands. Irradiation caused only a slight change and that occurred only in the control sample. The change seemed to indicate an irradiation induced level somewhere between 0.25 and 0.1 eV from a band edge.

2.1.5 Room Temperature Annealing. After 17 hours of annealing at room temperature, a statistically significant portion of the acceptors had not annealed. As a result, no estimate can be given for the number of lithium ions required to neutralize each acceptor. Preliminary measurements made at 76 hours indicate such changes are ocurring.

Significant annealing of the 0.12 eV level has taken place, and is shown in Figure 8. The measured activation energy for this level in each sample is shown in the top figure, and the measured concentration in the lower. In the phosphorus-doped sample the activation energy of this level remains constant upon annealing. Annealing does cause an initial increase in the concentration, but after 2 hours, this too becomes constant. In the lithium doped sample, however, annealing at 300^{o}K initially causes the 0.12 eV level to shift deeper into the gap, after which the activation energy remains fairly constant. This is consistent with the observations of the previous experiment. During this time, the concentration of this level in

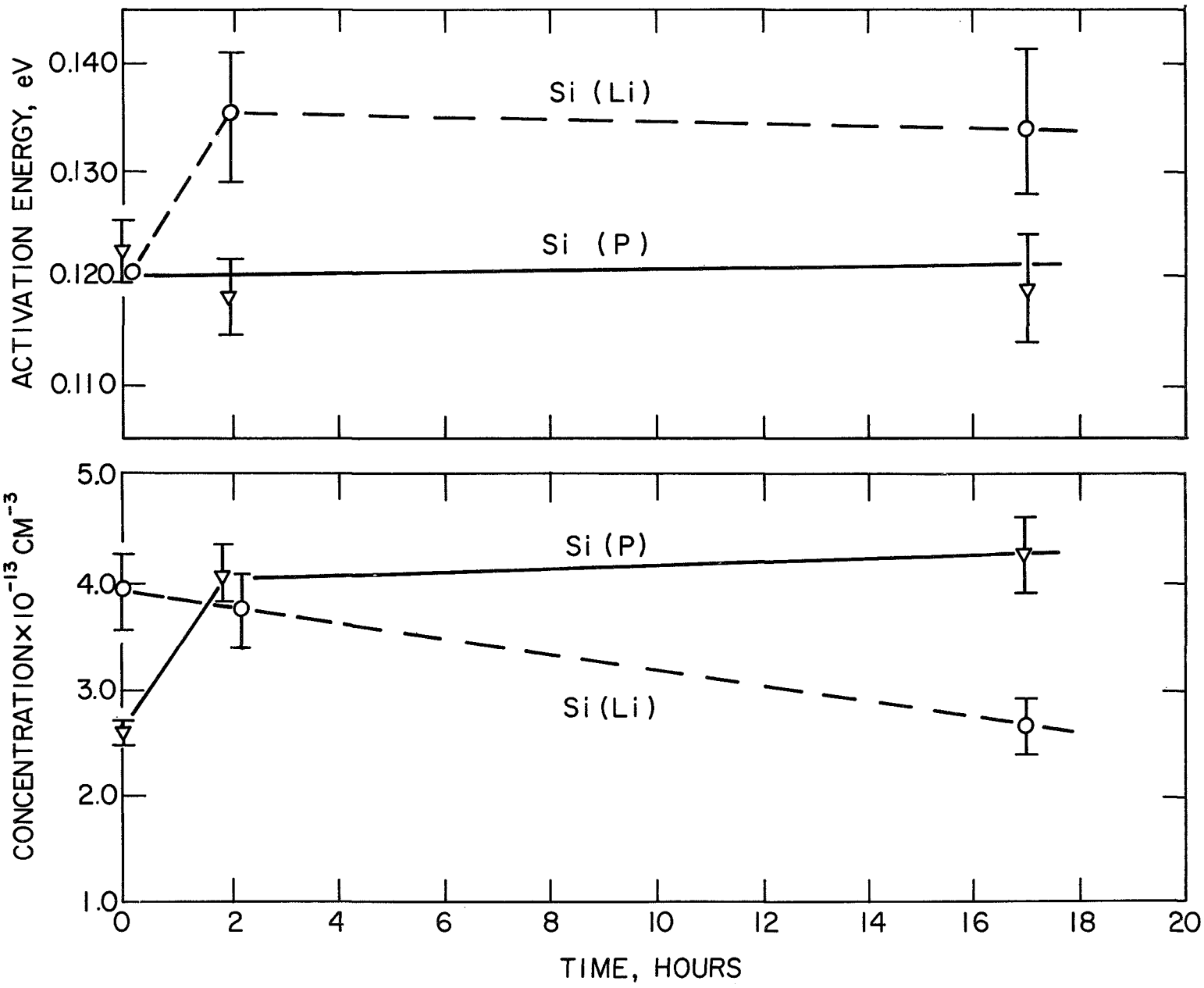

Fig. 8 - Effect of mobile lithium upon a radiation-induced level at E_c-.12 eV.

the lithium doped sample is steadily decreasing. It would seem probable that the energy shift must be due to the presence of lithium.

An important point is that the shift in the level occurs rapidly and goes to completion in a time during which few of the centers are rendered electrically inactive. This implies that neutralization occurs in two stages. For example, one or more lithium ions may be attracted to the center relatively quickly to form some sort of stable configuration. The final neutralization may then be rate-limited by effects associated with the microscopic nature of the defect.

2.2 Real-Time Irradiation of Lithium-Doped Solar Cells

2.2.1 Introduction. Lithium diffused into p/n silicon solar cells as an added dopant is well known to give to the cell the property of self-recovery from radiation damage. The amount of the recovery, and the rapidity of this process, depends largely on the concentrations of certain impurities in the silicon, the kind of radiation, the radiation dose, and the ambient temperature of the cell following the irradiation. Almost all radiation experiments with lithium-doped solar cells have been performed with particle accelerators which generate radiation fluxes that are several magnitudes greater than space radiation flux. Since no experimental evidence indicates whether the recovery of the lithium doped solar cell is dependent on the rate of radiation damage, it is important to study the damage and recovery processes at low flux rates as well.

2.2.2 Design of the Experiment. In order to evaluate radiation damage in solar cells which are exposed to radiation with an intensity comparable to space radiation fluxes, the NRL Cobalt-60 gamma pool source was utilized. The intensity of the radiation at the point where the experiment is located was 4.8×10^3 roentgen/hour at the start of the experiment in September 1969. The strength of the source decreases about 1% per month because of the natural radioactive decay of Co^{60}. The kind of damage caused by the ~1.2 MeV Co^{60} gamma ray is produced by an orbital electron in the silicon becoming highly energized by a gamma photon in a Compton scattering process. This energetic electron creates lattice displacements in the silicon with the subsequent formation of defects and centers similar to those which occur in electron-irradiated silicon. A first approximation for equivalency of damage in solar cells from Co^{60} gammas as compared with electrons can be made on the basis of determining the number of gamma photons which will produce the same number of lattice displacements as a 1 - MeV electron. Using values[6] for the total number of displaced Si atoms per unit of incident flux of 10^{-2} for 1 MeV gamma photons and 4.6 for 1 MeV electrons, the equivalent electron dose corresponding to 1 rad (Si) which is 2.22×10^7 photons/cm^2 is then 4.35×10^6 e/cm^2. This equivalency factor is applicable only when the gamma environment is one of electronic equilibrium for the irradiated sample. In the case of this particular experiment, where the cells are mounted on 1/8" thick brass plates, the extent of deviation from electronic equilibrium can be calculated*.

First, one may calculate the absorbed dose in a solar cell which is considered to be in radiation equilibrium. This condition would exist for a silicon cell encased in silicon in all directions. In this case

*This calculation for absorbed dose in the solar cells in this experiment was performed by F.H. Attix.

$$\text{Absorbed Dose (Rad) Si} = 0.869 \times \frac{(\mu_{en}/\rho)\ \text{Si}}{(\mu_{en}/\rho)\ \text{air}} \quad (1)$$

where μ_{en}/ρ is the mass energy-absorption coefficient (cm^2/gm)[7] of the specified material for 1.2 MeV gamma photons, and 0.869 is the absorbed dose (rads) in dry air produced by one roentgen of gamma irradiation. The strength of the gamma source in roentgens was previously determined at each compositon by ferrous sulfate dosimetry to an accuracy of ±1/2 percent. This becomes

$$\text{Absorbed Dose (Rad) Si} = 0.869 \times \frac{0.0265}{0.0266} \quad (2)$$

$$= 0.866 \ \text{Rad/Roentgen} \quad (3)$$

In the actual experiment, a correction must be applied to the absorbed dose because the solar cell is sandwiched between a 1/8 inch brass plate and a 0.018 inch stainless steel can wall. If the solar cell is a sufficiently thin material between two dissimilar materials (A and B), the absorbed dose may be approximated by the following expression:

$$\frac{\text{Actual Dose}}{\text{Equilibrium Dose}} = \frac{(\mu_{en}/\rho)\ \text{A-B}}{(\mu_{en}/\rho)\ \text{Si}} \times \frac{(S/\rho)\ \text{Si}}{(S/\rho)\ \text{A-B}} \quad (4)$$

where (μ_{en}/ρ) A-B is the average of the mass energy-absorption coefficients for materials A and B, (S/ρ) is the mass-stopping power $(MeV\text{-}cm^2/gm)$ for 300 KeV electrons (average energy for Compton electrons) in the specified material. Then

$$\frac{\text{Actual Dose}}{\text{Equilibrium Dose}} = \frac{(0.0248)\ \text{Cu-Fe}}{(0.0265)\ \text{Si}} \times \frac{(1.904)\ \text{Si}}{(1.664)\ \text{Cu-Fe}} \quad (5)$$

$$= 1.071 \quad (6)$$

The actual dose is calculated from the radiation field strength using expressions (3) and (6).

$$\text{Actual Dose (Rad) Si} = 0.866 \ \text{Rad/Roentgen} \times 1.071 \quad (7)$$

$$\text{Actual Dose (Rad) Si} = 0.93 \ \text{Exposure (Roentgen)} \quad (8)$$

Since the silicon solar cell is not thin enough to satisfy the conditions for a truly thin sample, we should consider the limits of accuracy of this calculation. It is evident that if the silicon were thick enough that a radiation equilibrium condition existed within, the actual dose at some interior point would be the equilibrium dose and the corrective factor becomes unity. Thus the value of 1.071 represents the upper limit of departure from radiation equilibrium. Therefore we can assume that the actual dose probably lies within a factor of 1.04 ± 3% of the equilibrium dose. This is better accuracy than is usually associated with electron flux dosimetry using Faraday cups for Van de Graff.[5]

2.2.3 Description of the Apparatus. The solar cells are of five types. There are four groups of Heliotek lithium-doped p/n cells, and a group of Centralab 10 ohm-cm n/p flight quality cells. Table I shows the experimental matrix for this study. The lithium-doped cells were obtained through JPL, and the N/P cells were obtained directly from Centralab.

Three stainless steel cylindrical cans about 3 in. diameter and 9 1/2 in. long are used for the irradiation and environment chambers for the cells. The solar cells are held against brass plates by spring clips at the main bus bar. Each cell is loaded with a ten-ohm resistor, with electrical contact being made through the spring clips and brass plate, as shown in Fig. 9. Illumination is provided by five automobile type lamps in each can, placed as depicted in Figure 10. After loading the solar cells, the cans are evacuated and then back filled with 1 psi of argon for the environmental exposure.

The cell temperatures are maintained by controlling the temperature of the brass plate by means of electrical strip heaters and water-carrying tubing soldered to the back of the plates. One can is held at 30°C, and two cans at 60°C with a variation of ± 1°C. The cells are removed from the cans for measurement of their I-V curves under illumination from a Spectrosun X-25L solar simulator at 140 nW/cm^2 air mass zero conditions at periodic intervals.

2.2.4 Results and Discussion. The experimental results at the end of seven months of testing will be discussed. During this time the solar cells were removed from the source and measured five times. From three to five solar cells of each group were exposed to each set of experimental parameters, in order that a satisfactory statistical evaluation of the results could be made. In almost all cases, this proved to be a sufficient number of samples so that the standard deviation of each set of data was less than ± .02. The data outside this limit occurred in the H-5 and H-9 groups. In the case of the H-5 cells, the low lithium-diffusion temperature during manufacture resulted in cells which, by capacitance measurement, contained almost no lithium at the junction. It is not surprising that the radiation data for these cells exhibited greater scatter than for the other groups. However, the unirradiated 60°C control cells in this group had self-consistent behavior. In the case of the H-9 cells, the contacts on four

TABLE I Co^{60} EXPERIMENT SAMPLE MATRIX

Cell Group	Type	Li Diffusion Parameters	Number Irradiated Controls		
			30°C Illuminated	60°C Illuminated	60°C Illuminated
H-2	Li P/N Crucible	90 min 425°C- 60 min 425°C	5	5	3
H-6	Li P/N Crucible	90 min 450°C- 60 min 450°C	5	5	3
H-5	Li P/N Float Zone	90 min 350°C- 60 min 350°C	5	5	3
H-9	Li P N Float Zone	90 min 425°C- 60 min 425°C-	5	5	3
Centralab	N/P Crucible	N.A.	5	5	3

All lithium-doped cells were made by Heliotek.

All cells are illuminated with tungsten light and are individually loaded with a 10 ohm resistor, developing a load voltage of 0.21 to 0.24 volt.

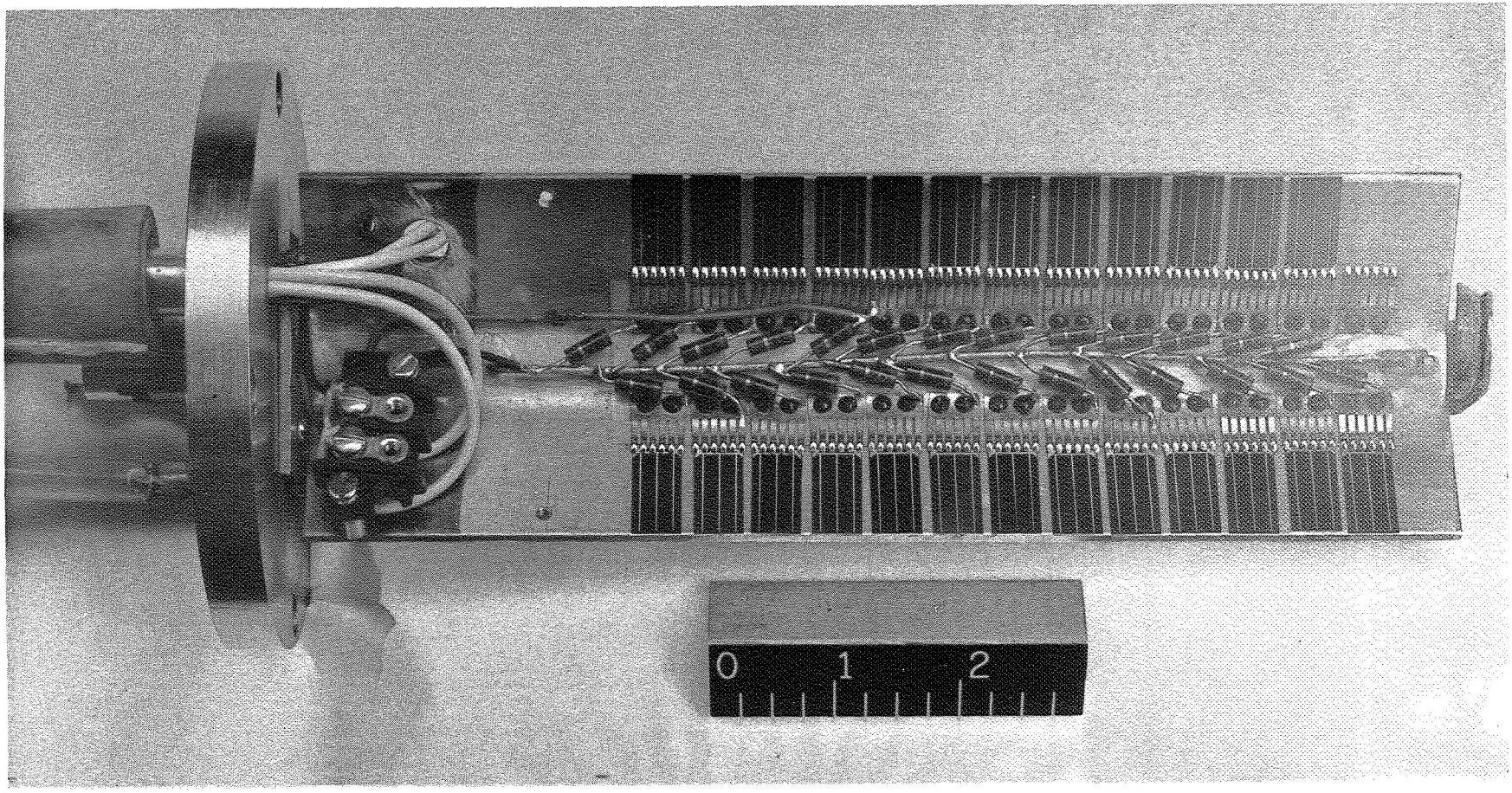

Fig. 9 - Solar cells are held against brass plate by pressure contacts for Cobalt-60 gamma irradiation. Each cell is loaded by a ten-ohm resistor.

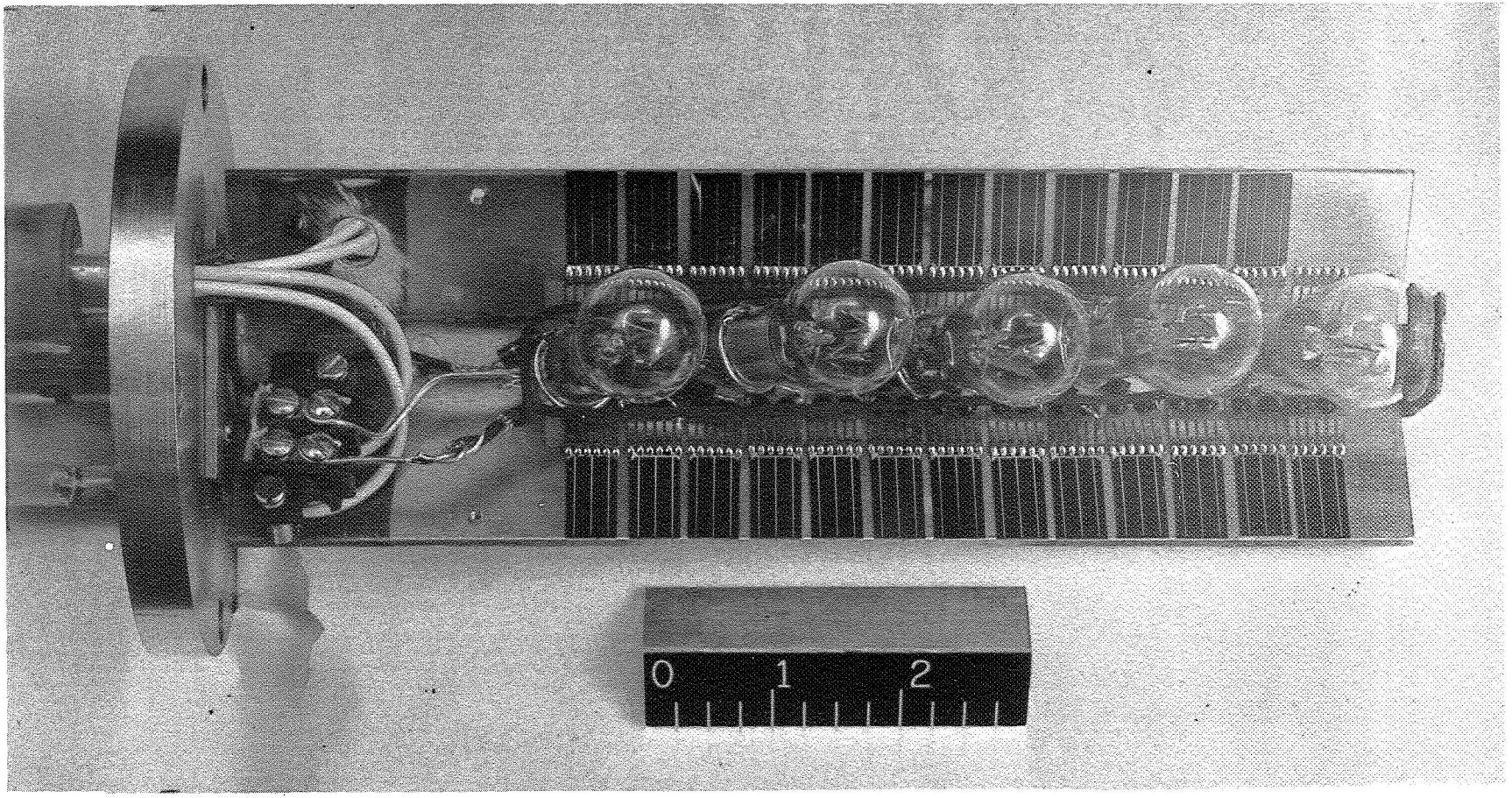

Five 12-volt lamps operating at 1.1 amperes illuminate the solar cells for the Cobalt-60 gamma experiment.

of the five irradiated 60°C cells failed at progressive intervals over the seven month period, so that only data for one cell at 60°C irradiation is given. In Table II are presented the results of the photovoltaic measurements comprising the initial short-circuit current, maximum power, and efficiency for each group of cells. Then the relative maximum power P/P_o (same value as relative efficiency) is listed for the case of 60°C and 30°C irradiation, and 60°C control cells. This data was obtained following a gamma dose of 2.3×10^7 roentgen, equivalent to 0.93×10^{14} e/cm^3.

The absolute values of maximum-power are plotted in Fig. 11 for the pre-radiation and for the post-irradiation measurements after seven months. This graph shows that none of the lithium-doped cells have an output power as great as the conventional n/p 10 ohm-cm solar cell in this environment, suggesting that no advantage has been found for diffusing lithium into p/n cells at these particular diffusion schedules and temperatures. The data in Fig. 11 also reveal that the temperature of the cells during irradiation does influence the amount of observed damage, since all groups of cells irradiated at 60°C are slightly more damaged than those at 30°C. There is also a certain amount of power degradation among the two control groups of n/p cells and H-9 cells, which are held at 60°C without irradiation. The reason for this has not been determined. In the case of the n/p cells, this effect may be connected with contact degradation, rather than a change in the properties of the silicon or p-n junction. The cause for this deterioration in the lithium float-zone cell could be related to the increased diffusivity of lithium with increased temperature, affecting either the internal properties of the cell or the contacts.

Fig. 12 is a plot of relative maximum power (P/P_o) as a function of equivalent 1 MeV electron fluence. Only the H2 and H9 groups of lithium cells are shown, because they were the more radiation resistant at 30°C. While the n/p cell and the quartz-crucible lithium cell have nearly equal degradation rates, the float-zone lithium cell degrades much more slowly.

It is not certain whether the greater damage rate in the H2 QC cells is due to the formation of unannealable damage centers, or whether the time constant for annealing of damage by lithium is greater than the radiation defect introduction rate. The float-zone material seems to produce a device which is more responsive to the annealing process under simulated real-time radiation fluxes.

TABLE II PHOTOVOLTAIC PARAMETERS OF EXPERIMENTAL CELLS

Cell Group	Type	I_{sc} mA	P_{max} mW	Efficiency	Relative P_{max} after 2.3×10^7 r+		
					Control	Irradiated	
					60°C	60°C	30°C
H-2	Lo Li CG	64.5	27.8	9.9	1.01 ± .02	.89 ± .02	.90 ± .02
H-6	Hi Li CG	60.0	24.7	8.8	1.01 ± .01	.92 ± .02	.92 ± .02
H-5	Lo Li FZ	70.0	27.4	9.8	.99 ± .02	.83 ± .07	.85 ± .03
H-9	Hi Li FZ	61.0	25.1	9.0	.93 ± .01	(.86)*	.95 ± .02
N/P	10 ohm-cm	71.5	29.2	10.4	.98 ± .01	.89 ± .01	.90 ± .01

+Equivalent to 1.03×10^{14} 1 MeV e /cm^2

*Only 1 cell remaining at this dose

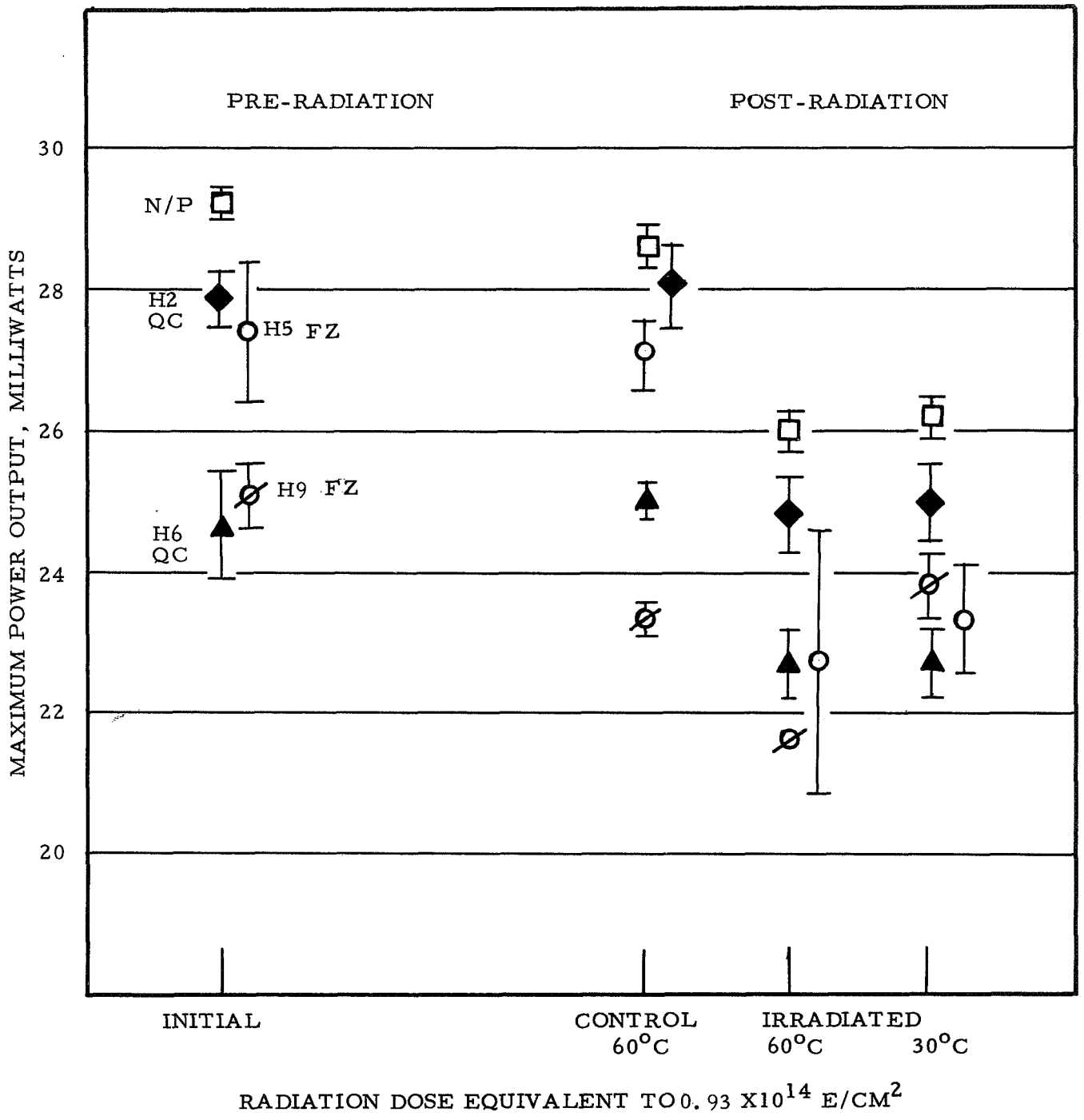

Fig. 11 - The maximum power output of five types of solar cells before and after Cobalt-60 irradiation. The illumination on the cells was 140 mW/cm^2 AMO from a solar simulator.

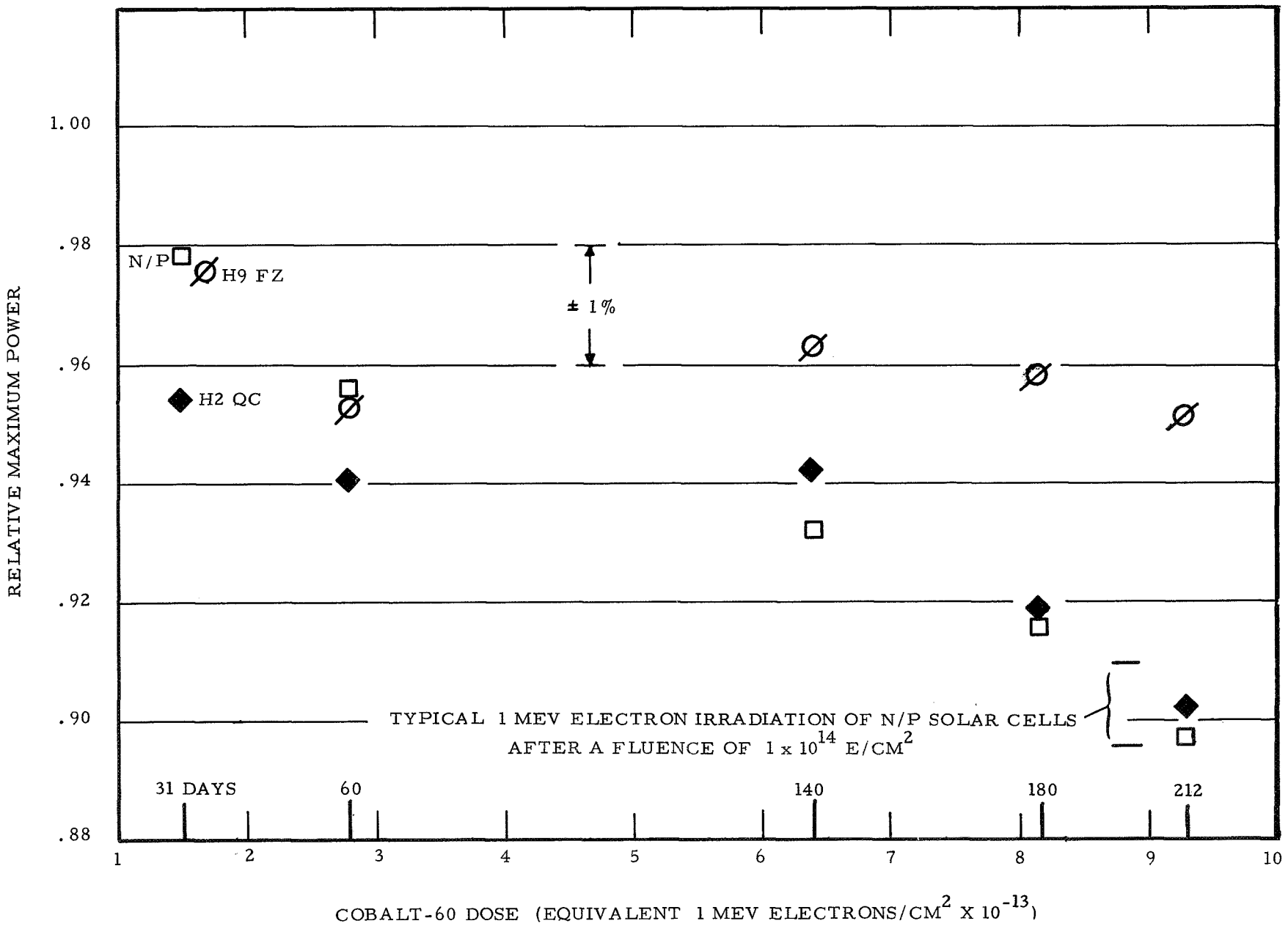

Fig. 12 - Relative maximum power output of three types of solar cells as a function of Cobalt-60 irradiation.

2.3 Radiation Damage of Silicon Solar Cells at Low Temperatures

2.3.1 Introduction. A program is in progress to determine the temperature dependence of radiation damage in solar cells due to electrons. This is part of a continuing program to investigate the behavior of solar cells in an environment which might be encountered on a deep space probe to the outer planets. This knowledge is necessary for proper system design if it is decided to use solar cell power systems on these missions.

There are several problems which are encountered when operating solar cells at both low temperatures and low intensities. (The Jupiter environment, for example, would require the operation of cells at 140°K and 5 mW/cm^2 solar intensity.) First, the diode term in the solar cell equation becomes more important as temperature decreases. This is particularly true at low intensities. Thus, it is desirable to select cells with low dark current values. At low intensities the effective series resistance is less important than at higher intensities.

On the other hand, there are several advantages to operating cells at low temperatures. As the temperature of the semiconductor is lowered, the energy gap becomes wider and the Fermi level moves closer to the valence band in p-type material and moves toward the conduction band in n-type material. These two effects combine to give increased open-circuit voltage at low temperatures and thus increase photovoltaic conversion efficiency in solar cells. An illustration of the temperature dependence of the energy gap and Fermi level is given in Fig. 13. The wider band gap also means that the creation of electron-hole pairs occurs at a higher energy threshold and results in a shift towards the blue end of the spectrum (and therefore, towards the peak in the solar spectrum). This is shown experimentally in Fig. 14.

The unknown factor in the operation of cells at low temperatures is the effect of irradiation. In order to investigate the effects of temperature on damage rate, a group of 25 Heliotek 10 Ω- cm cells, which were fabricated from the same boule of silicon, were selected for the first study. Of these 25, 4 remain and useful data were obtained on 11 cells. The experiments and results are described below.

2.3.2 Description of the Experiment. The cells are mounted four at a time (two on the front and two on the rear) on a sample holder attached to the cold finger of a research dewar. The sample mount and dewar have been described previously[8]. The mounting configuration was designed to reduce sample strain when operating at low temperatures. A substrate of very high resistivity silicon is soldered to the copper sample holder with indium (which "flows" at temperatures as low as

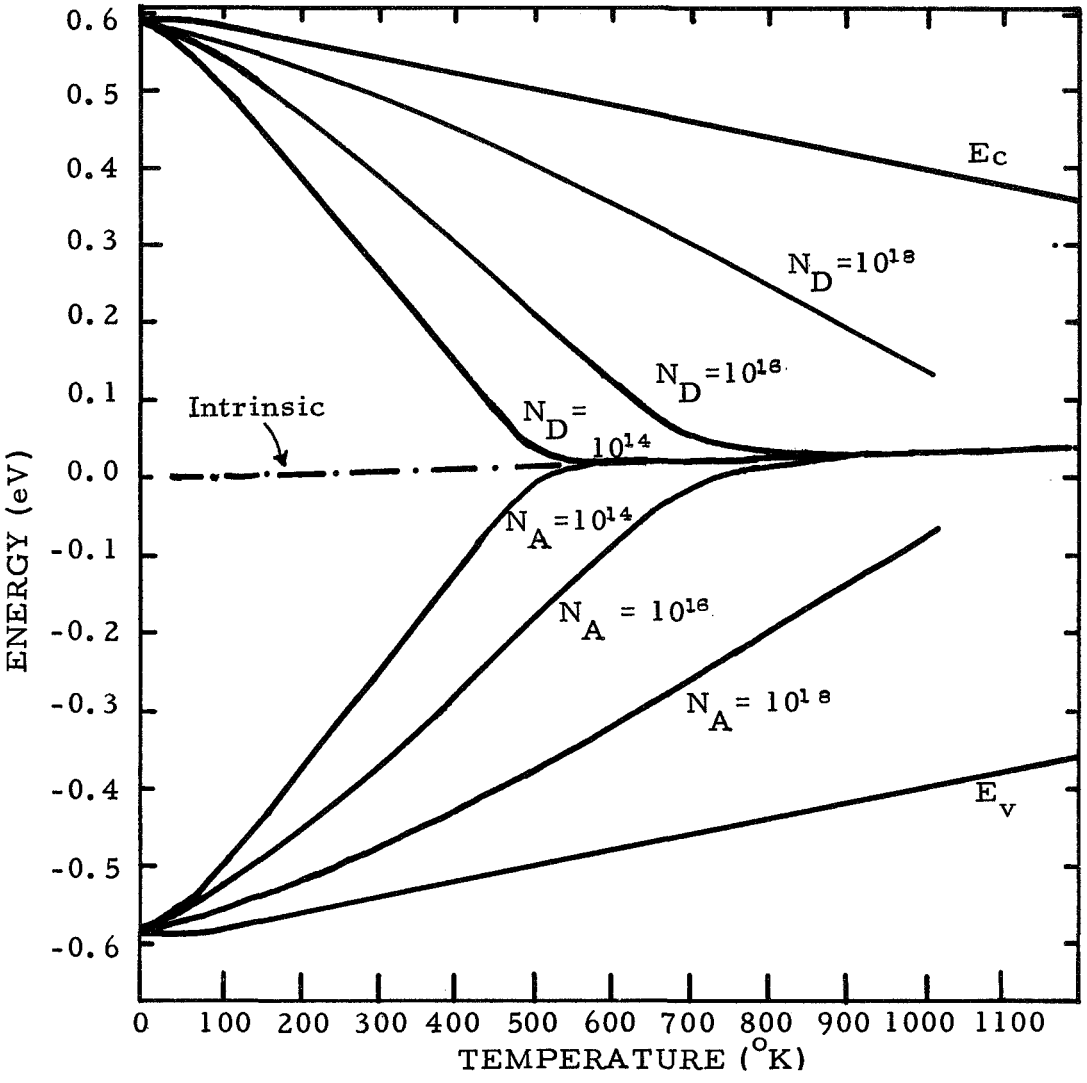

Fig. 13 - The positions of the Fermi levels in silicon as functions of temperature and impurity concentrations. Energies are measured from the center of the gap. The band gap is given by $E_g = E_c - E_v$.

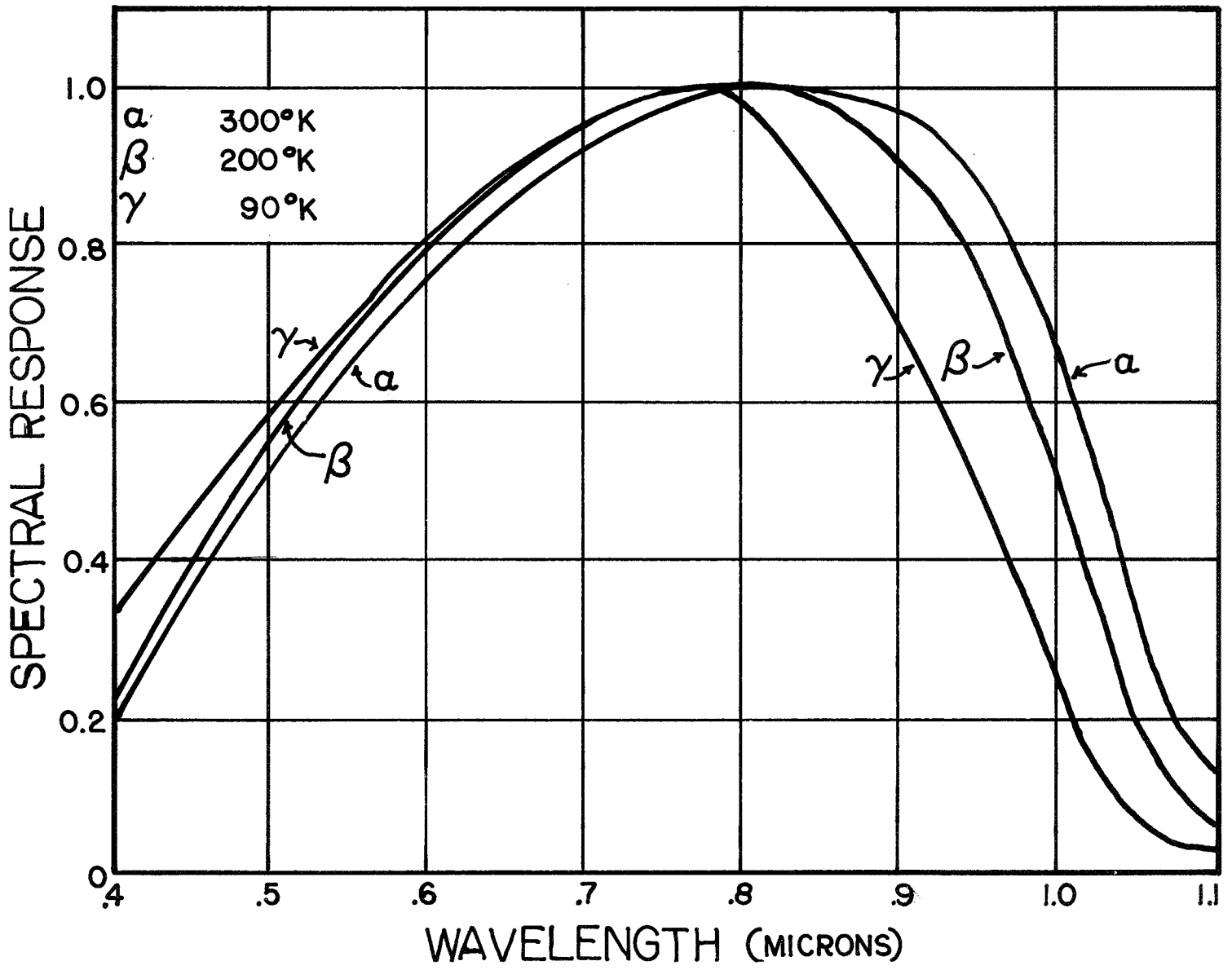

Fig. 14 - Relative spectral response as a function of temperature and wavelength.

77°K). The solar cells are then mounted on the silicon with G. E. varnish No. 7031. A thermocouple is soldered with indium to the bus bar of the cell and four leads (two current and two voltage) are also soldered to the cell.

I-V curves are obtained before and after each irradiation under illumination from a Spectrosun X-25 solar simulator. Each cell is successively irradiated to fluences of 10^{13}, 10^{14}, 10^{15}, and 5×10^{15} e/cm^2 at 1 MeV. Two cells are irradiated at one time because of space limitations. It has been determined through the use of silver-activated glass dosimaters[9] that the dosage received by the cells on the rear of the sample holder is at least two orders of magnitude less than that received on the front. Therefore, all four cells are mounted, and after irradiation of the first two, the beryllium window is rotated and the other cells are irradiated. The beam current is continuously monitored and integrated to determine the fluence. The dewar is equipped with a gate valve which permits the removal of the fused-quartz optical window during irradiation and prevents coloration of the window from irradiation. The temperature of the sample is monitored and is controlled to within 0.2°K by adjusting the current in the heater coil on the sample mount. During the course of the experiments it was found that the heater coil burned out whenever the current exceeded 90 ma. for a long period of time. This problem has been solved by installing another coil in parallel with the first. Prior to the installation of dual coils, two runs (8 samples) were aborted due to heater coil failure.

For each cell, I-V curves were obtained at 90°K so that cells irradiated at different temperatures could be compared.* These photovoltaic characteristics were measured under illumination intensities of 140, 100, 20, and 5 mW/cm^2 using neutral density filters to control intensity. Data were obtained for irradiation temperatures of 100, 125, and 300°K. In addition to the 90°K curves, data at 125° and 5 mW/cm^2 were obtained for the cells irradiated at 125° while measurements were made at all intensities at 300° for the cells irradiated at 300°K. All of the cells used in the experiment were quite uniform in their pre-irradiation characteristics. The current ranged from 62 to 64 m.a. at 450 mV AMO illumination.

2.3.3 Results and Discussion. Figure 15 contains the I-V curves for a representative cell which was irradiated at 125°K and measured at 90°K. The curves in Fig. 15 (a) were measured under illumination of 100 mW/cm^2, while those in Fig. 15 (b) were measured at an intensity of 5 mW/cm^2. The curves in Fig. 16 are for a "bad" cell under the same conditions. Notice that it would be impossible to predict from the high intensity curves that this cell would be so poor at low intensities. Since the dark current for these cells was not measured, it is not known whether cell No. He-10-10 differed appreciably from He-10-12 in this respect. This does illustrate, however, that I-V curves at high intensity - even at low temperatures are not a reliable test to select cells for low temperature use.

*A suggestion by G. Brucker in this regard is acknowledged.

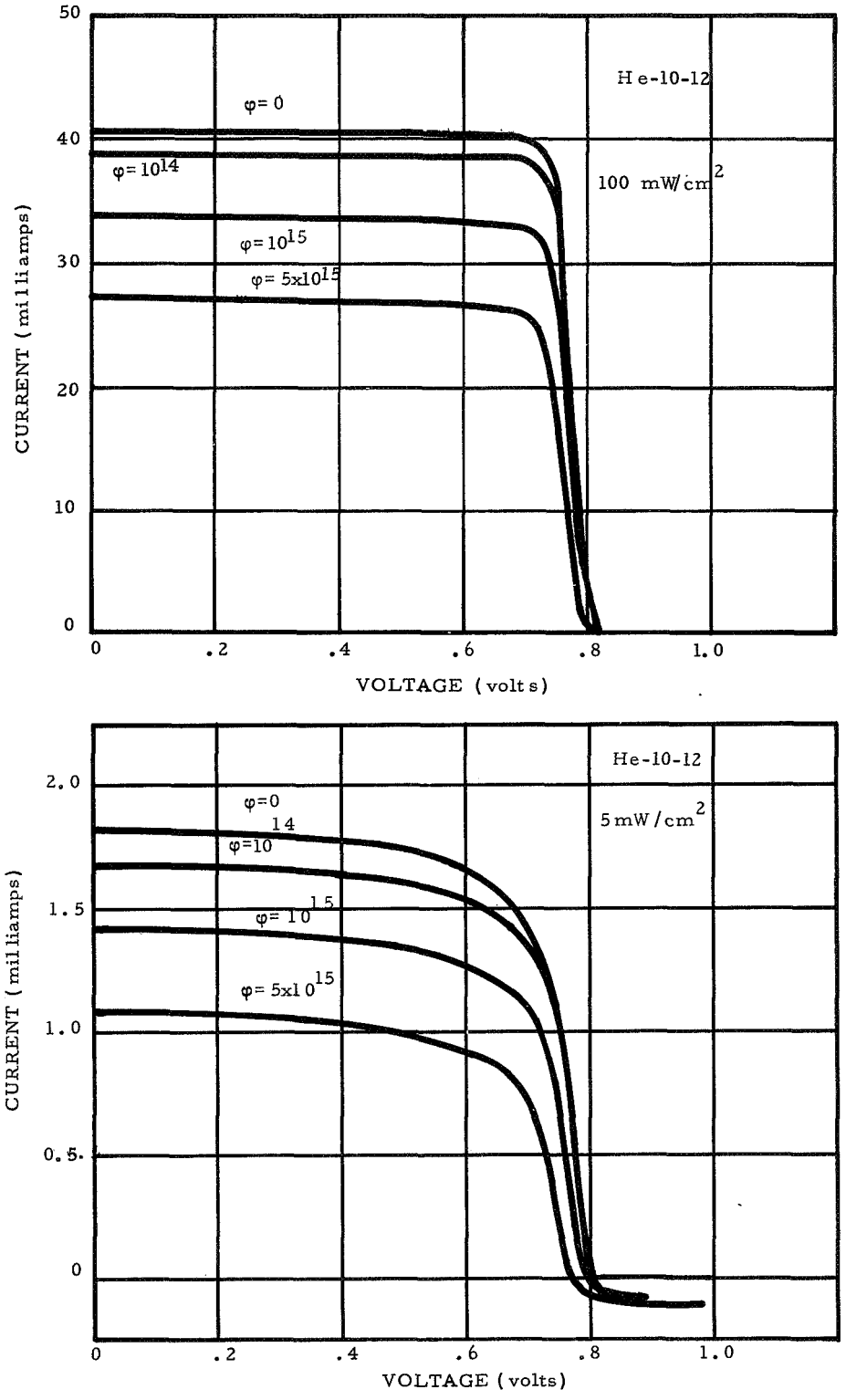

Fig. 15 - Current-voltage characteristics for a representative cell as a function of 1 MeV electron fluence. The cell was irradiated at 125°K and measured at 90°K under solar simulator illumination of (a) 100 mw/cm^2, and (b) 5 mw/cm^2.

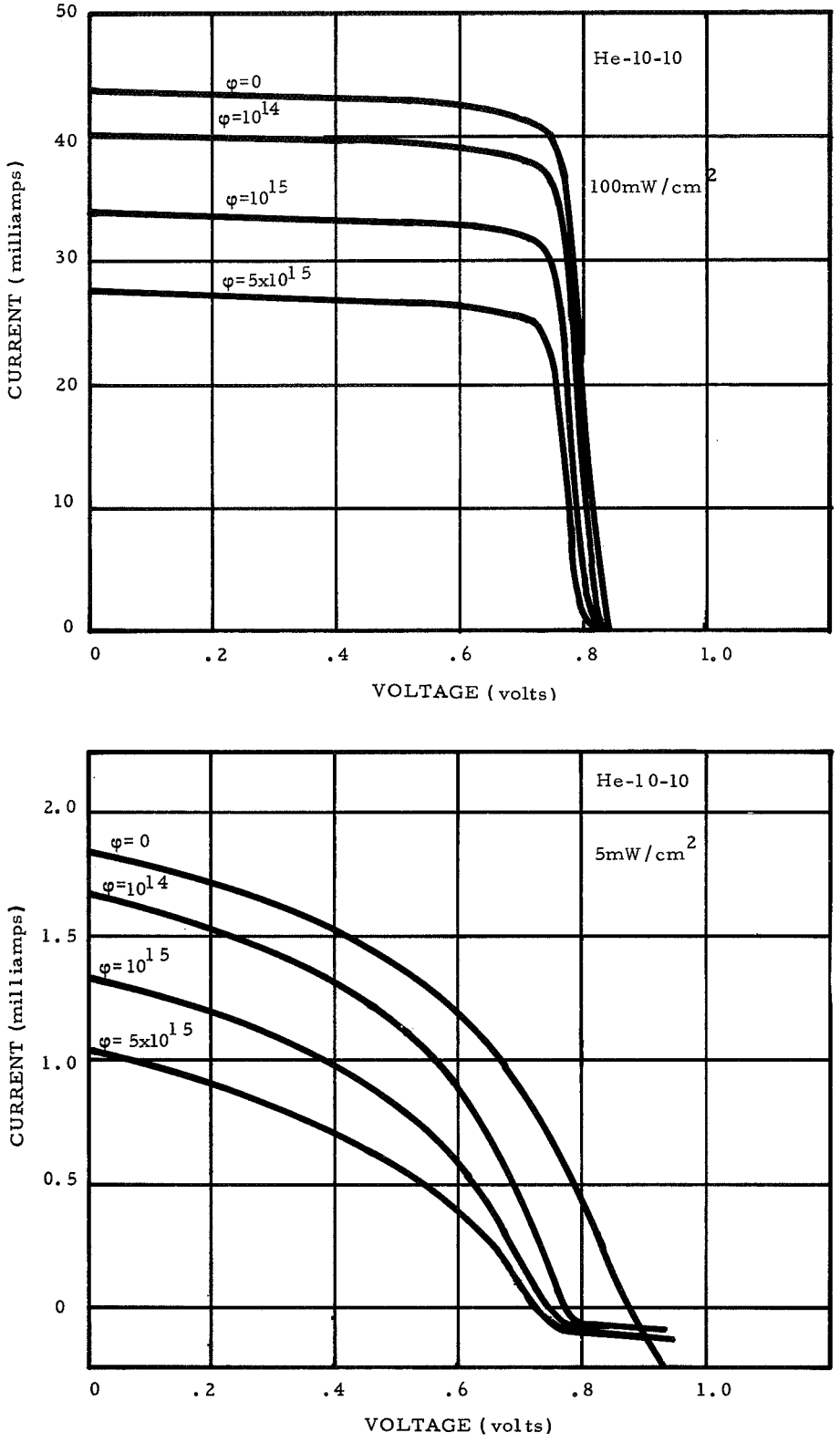

Fig. 16 - Current - voltage characteristics for a "bad" cell as a function of 1 MeV electron fluence; irradiations were performed at 125°K and measurements were made at 90°K under solar simulator illumination of (a) 100 mw/cm^2, and (b) 5 mw/cm^2.

It should be noted that the "tail" near open-circuit, which has been attributed to a "Schottky barrier" at the back contact, was present on all cells in this series of experiments at low temperatures. This effect drastically reduces the efficiency, as pointed out by P. Payne[10], who has shown that cells with a p^+ doping at the back contact do not exhibit the "tail" and develop open-circuit voltage which approach the theoretical value. It is not known whether p^+ doping will maintain the high efficiency of these cells after irradiation. Efficiency as a function of fluence and light intensity is given in Fig. 17 for cells measured at 90°K and irradiated at 125°K (Fig. 17 a) and at 300°K (Fig. 17b). It is evident that there is no apparent irradiation-temperature dependence on efficiency degradation rates, but the dependence of efficiency on intensity of illumination is rather large.

The behavior of short-circuit current for cells irradiated and measured at various temperatures is shown in Fig. 18. The ratio of short-circuit current after irradiation to short-circuit current prior to irradiation is plotted as a function of fluence. A comparison of the cells irradiated at 300°K and measured at 90°K with those cells irradiated at 125°K and measured at 90°K indicates that there is less degradation to minority-carrier lifetime at 125°K than at 300°K. On the other hand, a comparison of cells irradiated at 300°K and measured at 90°K with those same cells measured at 300°K indicates that the magnitude of this degradation is strongly dependent on measurement temperature.

A possible explanation of the data is, that during irradiation, stable defects are formed which have levels below the center of the band gap. These centers must act as donors, i.e. they are neutral at 300°K and are charged at 90°K. A likely candidate for this is the divacancy which appears to have a donor level in p-type silicon at about 0.25 eV above the valence band.[11] For 10 Ω - cm material the Fermi level is at E_v + 0.23 eV at 300°K and at E_v + 0.08 eV at 90°K. The 0.25 eV level would, therefore, be thermally occupied (and neutrally charged) at 300°K. At 90°K, this level would be nearly "frozen out" and the level would be positively charged and have an enhanced interaction cross section for electrons.

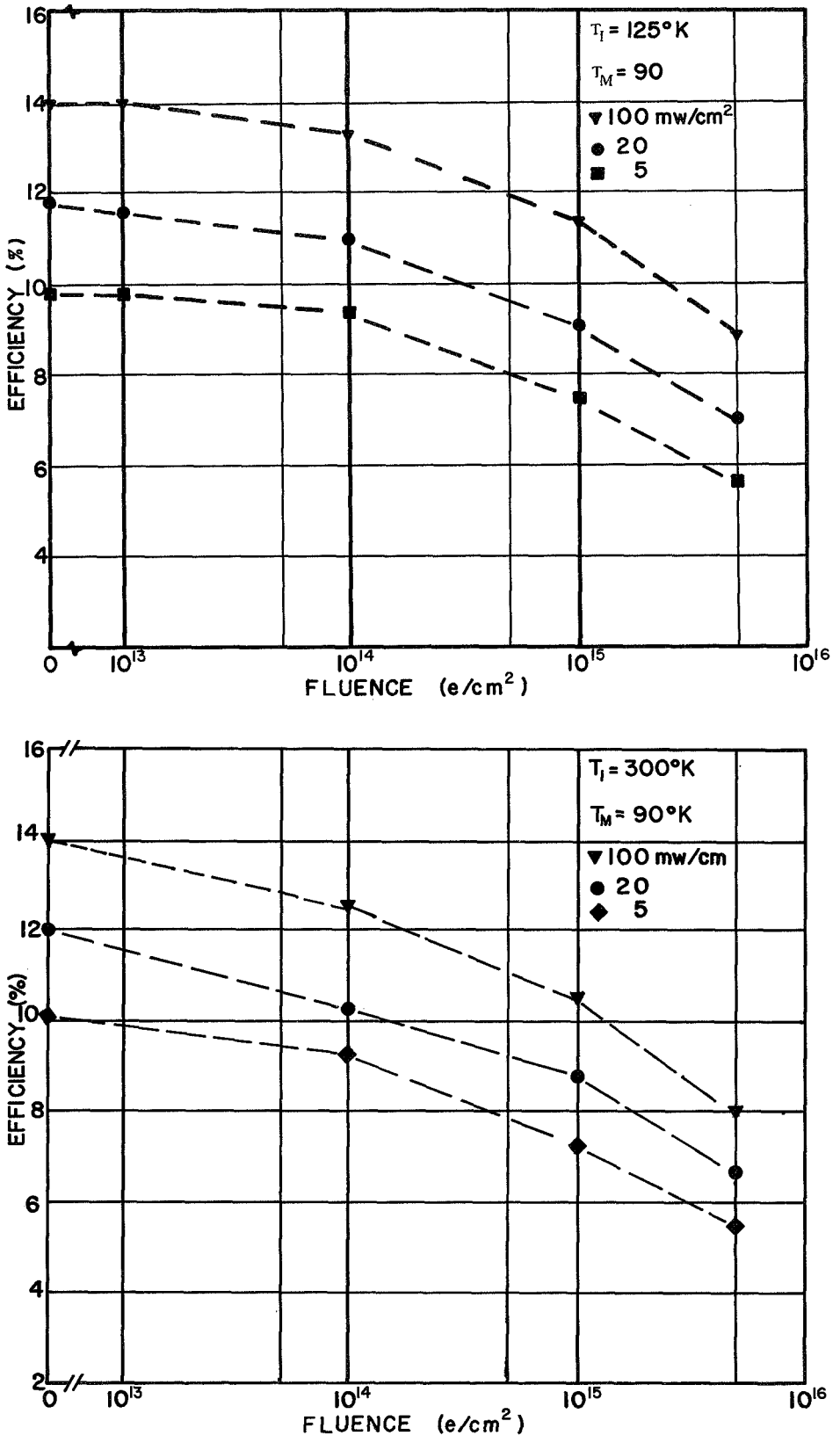

Fig. 17 - Efficiency as a function of 1 MeV-electron fluence and illumination intensity. The cells were irradiated at (a) 125°K and (b) 300°K and measured at 90°K.

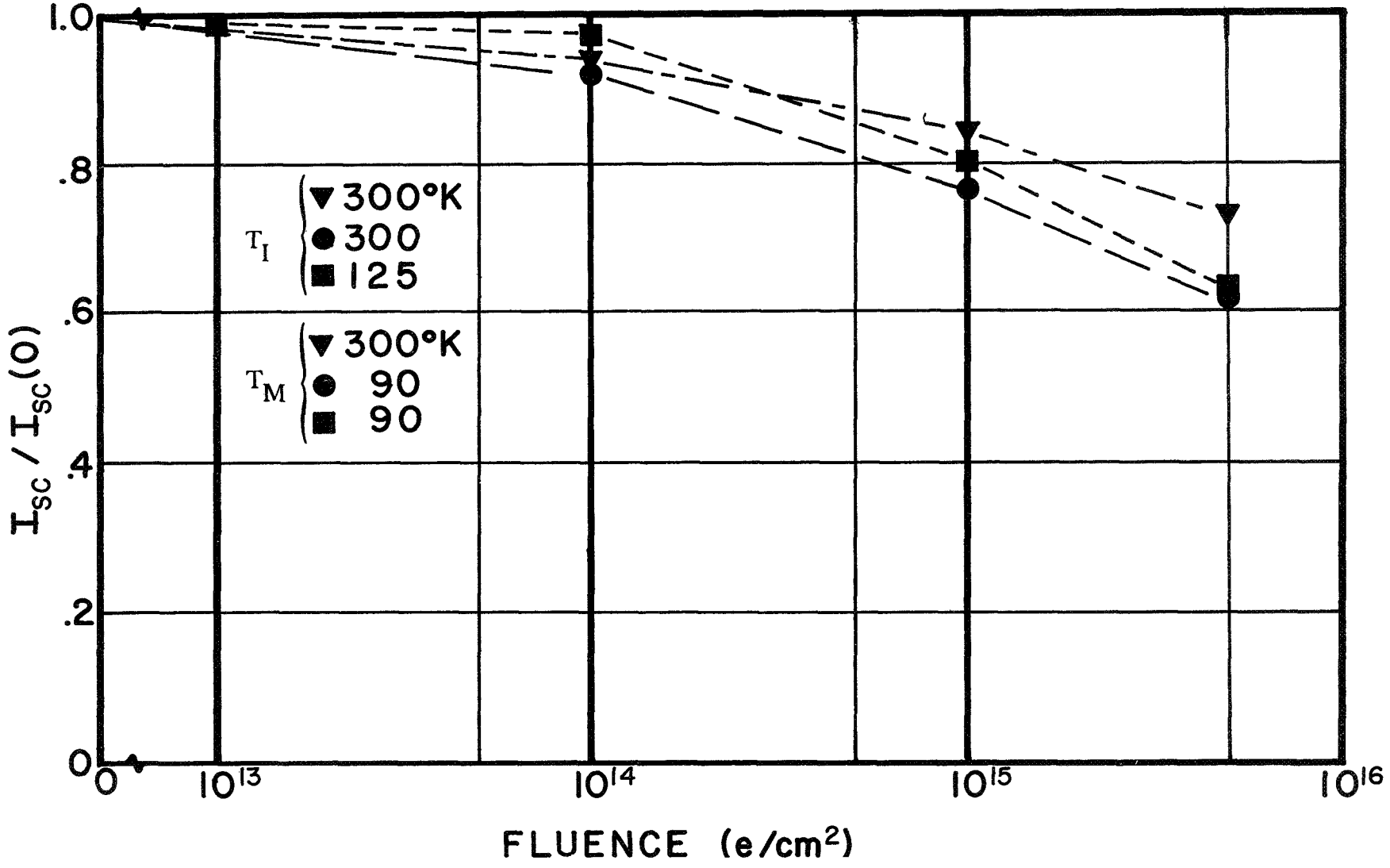

Fig. 18 - Normalized short-circuit current as a function of 1 MeV electron fluence for various irradiation and measurement temperatures.

3.0 CONCLUSIONS

A. In the Hall effect studies, quite good success has been achieved in computer-fitting the data to a two-impurity level model. The excellent results are due in part to more precise temperature measurement, but largely to improved sample preparation techniques. The diffusion of lithium into the silicon wafer from two sides, and the modified "tack-on" - etch-redistribution cycle result in better uniformity of the lithium profile and well-controlled concentration.

In 1 MeV electron bombardment, the lithium-diffused float-zone wafers showed greater damage than the phosphorus-doped control. While there is slightly less production of E-centers in the lithium sample, there is a much larger production of deep acceptor centers. These deep levels are removed by prolonged room-temperature annealing.

During room-temperature annealing, definite evidence of the effectiveness of lithium in removing electrically-active centers was obtained. The damage level at E_c-0.12 eV first moved deeper into the gap (E_c-0.135 eV), and then decreased in concentration as annealing proceeded. In the phosphorus-doped silicon, the activation energy of this level remained essentially constant while its concentration increased rapidly during early stages of annealing. Additional investigation of this level must be done before making firm conclusions about the damage center.

B. The low-flux Cobalt-60 irradiation of illuminated cells proves to be a useful method for discovering how lithium-doped solar cells respond to long, continuous radiation environment. The validity of this approach is strengthened by the good agreement between this study of n/p solar cells and previous 1 MeV electron data. Also, the real-time dose rate, together with cell evaluation under solar simulation, provide a more realistic appraisal of the anticipated performance of solar cells in space applications.

The lithium cells in this study were manufactured prior to June 1969, when relatively high diffusion temperatures and short time-cycles were utilized. More recent lithium processing has resulted in higher efficiency cells. These four types of lithium-doped solar cells all had lower initial efficiencies (ranging from 8.9 to 9.9 percent) than the 10.5 percent n/p cells used in the study. The n/p cells continued to have higher output power throughout the 212 day exposure, culminating in an equivalent fluence of 0.93×10^{14} 1 MeV e/cm^2. The quartz-crucible cells, designated H-2 were the most radiation-resistant of the lithium groups at this time.

All cells in the experiment, including the n/p, show greater damage when irradiated at 60°C than at 30°C. This may not clearly be a temperature-dependence of radiation damage. There is some degradation of unirradiated n/p cells and lithium-diffused float-zone cells held at 60°C as controls. The nature of this thermally-induced damage is not known.

C. The low-temperature irradiation study of solar cells has shown the following:

The degradation of efficiency in nominal 10 Ω - cm n/p solar cells without p^+ doping at the back contact is only weakly dependent on the temperature of irradiation. For example, cells which were irradiated at 300°K and 125°K to a fluence of 5×10^{15} 1 MeV e/cm^2 show a degradation of 37 and 36 percent, respectively, measured at 90°K under illumination of 5 mW/cm^2. This compares with a decrease of 37 percent for cells irradiated and measured at 300°K under the same illumination. However, these cells all exhibit the Shottky barrier phenomenon at low temperatures and, therefore, are less efficient than cells with a p^+ doping at the back contact.

Since the appearance of the "Schottky barrier effect" in the current-voltage curves may mask a small temperature-dependence of radiation damage, one may examine a cell parameter which is radiation-dependent but less sensitive to junction and barrier properties. Such a parameter is the short-circuit current, which, being a function primarily of minority-carrier diffusion length, is a measure primarily of lifetime-damage in the silicon. The lifetime is not affected by the Schottky barrier. The data indicate that the damage rate is more dependent on the measurement temperature than the irradiation temperature. Further experiments can determine whether the damage is due to intrinsic damage centers (such as the divacancy) or that the damage centers which are most effective in reducing minority-carrier lifetime are related to impurities.

4.0 RECOMMENDATIONS

The significance of the E_c-0.12 eV level in the damage and annealing processes in Si(Li) must be clarified. A room-temperature irradiation will be performed to see whether this level will appear and, if so, how it interacts. So far the level has been found at both 80°K and 240°K irradiations. In order to strengthen the body of Hall data and conclusions presented herein, a study of several more Si(Li) float-zone wafers prepared in the same way will be made, provided a condensed form of the experiment can be done. The present results indicate that material preparation procedures are critical to the interpretation and understanding of the entire experiment. For example, it is suggested that the presence of neutral lithium is responsible for the large carrier-removal rate in Si(Li). Therefore the heat-treatment cycle for preparing this material will be studied in a well-planned, logical manner (e.g. long diffusion times, quenching rates). Other kinds of silicon crystals, such as Lopex and quartz-crucible, will come into the study eventually.

In the low flux Cobalt-60 experiment, some newer types of lithium-doped cells will be used. These will include cells made by long time, low temperature diffusion. The flux of the present experiment will be increased about four-fold, now that the degradation rate of the present cells has become quite small. Cells of the same type as used in the Cobalt-60 environment will be irradiated by the electron beam from a Van de Graaff for fast damage-rate studies. These samples will be permitted to anneal under illuminated, resistor-loaded conditions at 30°C and 60°C. These results will be compared to the gamma radiation data for the purpose of establishing related damage values.

In the low-temperature solar cell work, new cells with a p^+ layer at the back contact will be irradiated at several temperatures and measured under various intensities, similar to the conditions reported here. In addition, diffusion length measurements in cells by electron-beam injection will reveal the basic aspects of those radiation-induced defects which are dependent on the measurement temperature. Also, the temperature-dependence of damaged cell spectral response will be studied during the next reporting period.

5.0 ACKNOWLEDGEMENTS

The dose calculations and analysis of the geometric factors in the Cobalt-60 gamma irradiation experiment were performed by F. H. Attix.

6.0 NEW TECHNOLOGY

1. Technique for uniform diffusion of lithium into a silicon wafer to a controllable concentration.

Originated by J. E. Stannard

Described in Semiannual Report for Solar Cell Research (Phase II), p. 2, 7 April 1970.

7.0 PUBLICATIONS

1. "Hall Effect Studies of Irradiated Si(Li) at Cryogenic Temperatures", J. E. Stannard, for the Proceedings of the Conference on Physics and Application of Lithium-Diffused Silicon, Jet Propulsion Laboratory, April 27-28, 1970.

2. "Real-time Irradiation of Lithium-Doped Solar Cells", R. L. Statler, ibid

8.0 REFERENCES

(1) E. L. Ralph, G. S. Goodelle, P. Payne, Investigation of Lithium Doped Hardened Solar Cells, First Quarterly Report, Contract No. AF 33-615-67-C-1458, Heliotek, August 1967.

(2) Morin, F. J., Maita, J. P. et al, Phys. Rev. 96, 833 (1953).

(3) R. L. Aggarwal, P. Fisher et al, Phys. Rev. 138, A882 (1965).

(4) R. L. Aggarwal and A. K. Ramdas, Phys. Rev. 137, A602 (1965).

(5) H. J. Stein & F. L. Vook, Phys. Rev. 163, 790 (1967).

(6) Transient-Radiation Effects on Electronics Handbook, DASA 1420, edited by R. K. Thatcher, Battelle Memorial Institute, p. E-4, August 1967.

(7) Radiation Dosimetry, Vol. I Fundamentals, edited by F. H. Attix, W. C. Roesch, and E. Tochlin, Academic Press, pp. 130-131, 1968.

(8) R. L. Statler et al, Annual Report for Solar Cell Research, Work Order 8056, Naval Research Laboratory, 15 October 1969.

(9) J. H. Schulman, C. C. Klick, and H. Rabin, Nucleonics, 13, 30 (1955).

(10) P. Payne, Research and Development of Silicon Solar Cells for Low Solar Intensity and Low Temperature Applications, First Quarterly Report, Contract No. NAS 2-5519, Heliotek, 15 October 1969.

(11) L. D. Konozenko, A. K. Semenyuk, V. I. Khivrich, and G. A. Dobrokhotov, Soviet Physics - Semiconductors, 3, 130 (1969).